https://doi.org/10.5194/egusphere-2026-6675
Preprint. Discussion started: 4 November 2026
© Author(s) 2026. CC BY 4.0 License.

Sediment-dynamics indicators for assessing fluvial-memory controls on suspended-sediment routing and deposition in a valley-type reservoir

Piotr Gierszewski[1], Włodzimierz Juśkiewicz[1]*, Monika Szlapa[2], Magdalena Tutro[2], Paweł S. Hachaj[2], Daniel Strzelecki[3], Michał Habel[4]

[1] Institute of Geography and Spatial Development Polish Academy of Sciences;
Kopernika 19, 87-100 Toruń, Poland
email: piotr.gierszewski@geopan.torun.pl, 0000-0001-5842-5157; w.juskiewicz@geopan.torun.pl, 0000-0002-6755-3975
[2] Faculty of Environmental and Power Engineering Cracow University of Technology;
Warszawska 24, 31-155 Cracow, Poland
email: monika.szlapa@pk.edu.pl, 0000-0001-5545-9036; magdalena.tutro@pk.edu.pl, 0000-0001-8191-4469; pawel.hachaj@pk.edu.pl, 0000-0001-5342-047X
[3] Faculty of Mathematics, Informatics and Mechanics, University of Warsaw; Banacha 2, 02-097 Warszawa, Poland
email: dstrzelecki@mimuw.edu.pl, 0000-0002-0006-3242
[4] Kazimierz Wielki University in Bydgoszcz; Kościeleckich Square 8, 85-033 Bydgoszcz, Poland
email: hydro.habel@ukw.edu.pl, 0000-0002-4661-6498

Correspondence to: Włodzimierz Juśkiewicz, (*w.juskiewicz@geopan.torun.pl*)

Keywords: Sediment-dynamics indicators; Fluvial memory; Suspended-sediment routing; Deposition stability; Redeposition; Valley-type reservoir; Reservoir sediment management

https://doi.org/10.5194/egusphere-2026-6675
Preprint. Discussion started: 4 November 2026
© Author(s) 2026. CC BY 4.0 License.



Abstract. River impoundment fundamentally alters hydraulic conditions and sediment-transfer processes, but the extent to which pre-impoundment fluvial morphology continues to structure sediment dynamics remains insufficiently quantified. In valley-type reservoirs, submerged channels, islands, bars and floodplain surfaces may preserve an inherited geomorphological template that influences contemporary flow pathways and depositional patterns. This study examines the persistence and sedimentary significance of this fluvial memory in the Włocławek Reservoir, a lowland through-flow reservoir on the Vistula River, Poland, more than five decades after impoundment. Reconstructed pre-dam morphology, measured bathymetry and suspended-sediment grain-size distributions were combined with two-dimensional hydrodynamic modelling (AdH) and Lagrangian particle tracking (PTM) under low-, medium- and high-flow conditions. Three dimensionless indicators—Relative Sedimentation Efficiency (RES), Sediment-deposition Stability Index (SDI) and Redeposition Index (RI)—were developed to quantify spatial contrasts in sediment capture, primary-deposit stability and secondary redistribution among inherited morphodynamic zones. Simulated sediment retention increased from 66% during high flow to 73% during medium flow and 94% during low flow. Former thalweg and island/bar zones exhibited disproportionately high sediment capture, with maximum RES values of 4.10 and 2.63, respectively, whereas former floodplain surfaces showed relatively low sedimentation efficiency. Higher flows reduced the stability of primary deposits and enhanced resuspension–redeposition processes. These findings indicate that inherited channel–island–floodplain morphology remains an important spatial organizer of sediment routing and deposition long after the transition from riverine to reservoir conditions. The proposed indicators offer a quantitative framework for investigating the sedimentary expression of geomorphological inheritance in valley-type reservoirs and for distinguishing depositional efficiency from sediment-storage stability.

1.Introduction

Rivers are dynamic systems whose present morphology and functioning reflect not only contemporary hydrological forcing but also the cumulative effects of earlier geomorphic, hydrological, and anthropogenic processes. Increasing attention has therefore been paid to fluvial legacy effects, understood as the persistence of inherited forms, deposits, and process domains that continue to influence contemporary river behaviour (Wohl, 2015, 2019; Buffington and Montgomery, 2022; Wohl et al., 2024). Such legacies may originate from extreme floods, discharge-regime shifts, long-term sediment-storage dynamics, or human modifications of river corridors, including channelization, land-use change, and hydraulic engineering (Livers and Wohl, 2016; Livers et al., 2018). Importantly, historical disturbances may produce persistent changes in channel morphology and functioning long after the original forcing has ceased, demonstrating that contemporary river conditions can remain strongly conditioned by past states of the system (Livers et al., 2018). They can be preserved in channel morphology, floodplain topography, alluvial deposits, and sediment-routing pathways, thereby influencing subsequent hydraulic conditions, sediment transport, and floodplain evolution (Sidorchuk, 2003; Buffington, 2012; Masteller et al., 2019; Hamidifar et al., 2024). In regulated rivers, dams introduce an additional form of geomorphic legacy by altering sediment transfer and creating sediment stores that may persist for decades to centuries (Livers and Snyder, 2025). Thus, river and reservoir systems may retain inherited morphological configurations that continue to organize contemporary hydrodynamic and sedimentary processes even after boundary conditions have fundamentally changed.

The capacity of dams to generate such long-term legacies reflects their fundamental alteration of river-system continuity. Dams alter flow regimes, hydraulic gradients, sediment supply, trapping conditions, and channel morphology, with effects extending both upstream into the impounded reach and downstream below the dam (Morris and Fan, 1998; McCartney et al., 2000; Timchenko et al., 2015; Gierszewski et al., 2020; Fang et al., 2024). Downstream, reduced sediment supply and modified flow conditions commonly promote channel incision, bed coarsening, and changes in channel geometry (Babiński, 2002; Habel, 2013; Gierszewski et al., 2015, 2020; Słowik et al., 2018). Upstream, reduced hydraulic gradients and flow velocities promote sediment trapping, grain-size sorting, delta development, and progressive reservoir infilling (Leopold et al., 1964; Morris and Fan, 1998; Liro et al., 2020). Classical reservoir-sedimentation concepts therefore emphasize longitudinal differentiation into riverine, transitional, and lacustrine zones, controlled mainly by inflow discharge, residence time, sediment supply, and decreasing transport capacity toward the dam (Thornton et al., 1990; Morris and Fan, 1998; Shotbolt et al., 2005).

However, reservoir sedimentation does not necessarily occur over a neutral or geomorphologically uniform substrate. In valley-type reservoirs, particularly those with short residence times and intensive throughflow, the inundated valley floor may retain a recognizable pre-impoundment morphology, including former thalwegs, secondary channels, islands, bars, and floodplain surfaces. These inherited elements can continue to structure flow paths, local velocity contrasts, sediment-routing corridors, and depositional patches within the reservoir (Venteris et al., 2014; Sedláček et al., 2016, 2022; Juracek, 2015; Keith et al., 2024; Stauch et al., 2024). In the Włocławek Reservoir, for example, previous studies have shown that the former Vistula channel still defines a preferential flow corridor and is reflected in contemporary sedimentation patterns, ice phenomena, and thermal conditions (Gierszewski, 2018; Hachaj et al., 2024).

https://doi.org/10.5194/egusphere-2026-6675
Preprint. Discussion started: 4 November 2026
© Author(s) 2026. CC BY 4.0 License.

The persistence of such inherited controls can be interpreted as a manifestation of fluvial memory. In this context, fluvial memory refers to the capacity of a river–reservoir system to preserve inherited morphological attributes and to maintain or reactivate their influence on flow pathways and sediment-routing structures under altered boundary conditions. Related phenomena and concepts have been described using terms such as river memory, fluvial memory, and morphological sustainability (Beevers, 2003; Hachaj, 2013; Iliopoulou et al., 2019; Ke, 2021). Hachaj (2013), for example, described the persistence of flow along the former river channel in the Goczałkowice Reservoir and proposed a physical explanation for this effect. Comparable mechanisms have also been observed after dam breaches or controlled reservoir flushing, when rivers incise into accumulated deposits and partly reoccupy former channel courses (Atkinson, 1996; Evans, 2007; Lai et al., 2024). These examples suggest that pre-dam valley-floor morphology may remain an active control on post-impoundment hydraulics and sediment dynamics rather than being merely a passive remnant of the former river system.

In the present study, fluvial memory is operationally defined as the preserved pre-impoundment morphological template of the Vistula valley that continues to influence contemporary hydraulic and sedimentary processes within the Włocławek Reservoir. This template includes the submerged former thalweg, secondary channel belts, former islands and bars, and marginal floodplain surfaces. These inherited elements are not treated as a general background characteristic of the reservoir, but as spatially explicit controls on the velocity field, suspended-sediment pathways, and the locations of primary deposition, resuspension, and redeposition. This definition does not imply a continuation of pre-impoundment riverine sedimentation; rather, it describes the persistence of an inherited spatial template that organizes sediment routing under fundamentally altered reservoir boundary conditions.

Although the persistence of pre-impoundment morphology has been recognized in several reservoirs, its quantitative influence on suspended-sediment deposition remains insufficiently resolved. Most reservoir-sedimentation models and conceptual schemes focus on hydrological controls, trapping efficiency, sediment supply, residence time, and longitudinal riverine–transitional–lacustrine zonation (Brune, 1953; Dendy and Champion, 1978; Thornton et al., 1990; Morris and Fan, 1998). Much less attention has been paid to whether inherited morphological elements of the inundated valley floor continue to organize suspended-particle trajectories, primary deposition, resuspension, and redeposition under variable flow conditions. This remains an important unresolved problem because predictions of depositional hotspots, sediment stability, sediment-trapping efficiency, and long-term reservoir-bed evolution may be incomplete if inherited morphological controls are ignored.

A related methodological challenge is the limited availability of indicators capable of translating spatially explicit hydrodynamic and sediment-transport simulations into diagnostic measures useful for reservoir assessment. Conventional reservoir-sedimentation metrics, such as trapping efficiency or longitudinal depositional zonation, provide valuable system-scale information, but they do not explicitly quantify where sediment capture is disproportionate to bed-area share, where primary deposits remain stable, or where secondary redistribution dominates. Such information is particularly relevant for through-flow reservoirs, where depositional hotspots, unstable sediment patches and resuspension-prone zones may affect habitat stability, turbidity dynamics, contaminant-associated sediment storage and sediment-management priorities.

The development of environmental indicators requires a balance between process complexity and interpretability. Indicator-evaluation frameworks emphasize that useful indicators should be conceptually relevant to the assessment question, feasible to calculate or measure, sensitive to meaningful spatial or temporal variability, and interpretable for assessment or management purposes (Kurtz et al., 2001). They should also capture key properties of complex systems while remaining sufficiently simple and integrative to support monitoring and comparative evaluation (Dale and Beyeler, 2001). In line with these principles, we developed three complementary, dimensionless indicators: Relative Sedimentation Efficiency (RES), Sediment-deposition Stability Index (SDI) and Redeposition Index (RI). Together, they reduce spatially explicit hydrodynamic and particle-tracking outputs to diagnostic measures of sediment-capture efficiency, depositional stability and secondary redistribution. They are therefore proposed as process-based hydromorphological indicators that can support reservoir assessment and sediment-management prioritization, while not replacing biological, habitat-quality or water-quality indicators.

The aim of this study is to investigate the persistence and sedimentary significance of inherited pre-impoundment fluvial morphology in a lowland valley-type reservoir. We hypothesize that the submerged channel–island–floodplain template continues to organize spatial patterns of suspended-sediment routing, primary deposition and secondary redistribution under contrasting hydrological conditions. To examine this hypothesis, we combine historical cartographic reconstruction and measured reservoir bathymetry with two-dimensional hydrodynamic modelling and Lagrangian particle tracking. We further introduce three dimensionless indicators—Relative Sedimentation Efficiency (RES), Sediment-deposition Stability Index (SDI) and Redeposition Index (RI)—to quantify differences in sediment capture, depositional stability and secondary redistribution among inherited morphodynamic units. The principal contribution of this study is to establish a quantitative relationship between preserved fluvial landforms and contemporary sedimentary processes, demonstrating how

https://doi.org/10.5194/egusphere-2026-6675
Preprint. Discussion started: 4 November 2026
© Author(s) 2026. CC BY 4.0 License.

geomorphological inheritance can remain functionally significant under fundamentally altered hydraulic conditions. This approach complements conventional longitudinal models of reservoir sedimentation by explicitly considering the spatial organization of inherited valley-floor morphology.
Particular attention is given to four research questions:
(i) how suspended-sediment routing and deposition differ among inherited morphodynamic zones;
(ii) how resuspension and redeposition modify primary depositional patterns under contrasting flow conditions;
(iii) how the spatial organization of sediment transport and deposition associated with the inherited channel–island–floodplain template varies across low-, medium- and high-flow scenarios; and
(iv) to what extent RES, SDI and RI provide complementary quantitative measures of sediment-capture efficiency, depositional stability and secondary redistribution across inherited morphodynamic zones.

2. Methods

2.1. Study area

The Włocławek Reservoir (WR), located in central Poland, was created in 1970 by impounding the lower Vistula River with the Włocławek Dam. In terms of surface area (75 km²), it is the largest reservoir in Poland and the second largest by volume (~370 million m³) (Gierszewski, 2018). The 1,200 m-long Włocławek Dam comprises a weir, an earth-fill embankment, a 160 MW hydropower plant, a navigation lock, a fish pass, and a lateral dike along the left bank.

WR has a morphology typical of valley-type reservoirs: it is narrow and elongated, with a weakly indented shoreline. It is 57 km long, with a mean width of 1.2 km and a mean depth of 5.5 m; maximum depths of about 15 m occur along the former Vistula channel, located mainly near the right bank (Gierszewski, 2018) (Fig. 1). As a consequence of impounding a sandy-bed multi-channel Vistula reach characterized by islands, bars and secondary channels, the reservoir bed exhibits pronounced bathymetric and morphological heterogeneity. Shallow areas are associated mainly with inundated bars, former river islands and low floodplain surfaces, especially on the left-bank side. This preserved morphology provides the physical template analysed in this study.

Table 1. Main pre- and post-impoundment characteristics of the Włocławek Reservoir relevant to sediment routing and inherited morphodynamic zonation.

Feature	Pre-impoundment Vistula reach	Present Włocławek Reservoir	Relevance to this study
System type	Sandy-bed multi-channel river reach	Long, narrow valley-type through-flow reservoir	Defines the inherited fluvial template preserved on the reservoir bed
Main morphological elements	Main thalweg, secondary/lateral channels, islands, bars and marginal floodplain surfaces	Submerged thalweg, remnants of secondary channels, former island/bar zones and inundated floodplain surfaces	These elements form the morphodynamic zones used in the analysis: TW — thalweg zone, representing the deepest former primary channel; RC — relict-channel/channel-belt zone, representing secondary and lateral channels; FRI — former island/bar zone; and FP — former floodplain zone
Water depth	Shallow and laterally variable river channel, with deeper zones along the active thalweg	Mean depth 5.5 m; maximum depth about 15 m along the former Vistula channel	Impoundment increased water depth, but the deepest corridor still follows the former thalweg
Flow conditions	Concentrated flow along the main and secondary channels; lower-energy zones around islands, bars and floodplain margins	Reduced average flow velocity relative to riverine conditions, but a persistent higher-velocity corridor remains aligned with the former thalweg	Indicates that present hydrodynamics are altered by impoundment but remain spatially organized by inherited morphology
Water residence time	Riverine throughflow without reservoir storage	Short mean residence time, approximately 5.2 days	Supports the interpretation of WR as a dynamic through-flow reservoir rather than a fully lacustrine basin
Sediment routing	Bedload and suspended load routed mainly	Nearly complete trapping of bedload and	Indicates that reservoir sedimentation is modified by

https://doi.org/10.5194/egusphere-2026-6675
Preprint. Discussion started: 4 November 2026
© Author(s) 2026. CC BY 4.0 License.

	through the channel belt; fine sediment deposited in lower-energy island-margin and floodplain environments	partial trapping of suspended load; deposition, resuspension and redeposition occur within inherited morphological zones	impoundment but remains spatially constrained by the former channel–island–floodplain template
Dominant inherited control	Channel–island–floodplain morphology of the pre-dam Vistula	Preserved bathymetric and morphological template on the reservoir bed	Provides the operational basis for analysing fluvial memory in this study

Table 1 contrasts the inherited morphological template with the present reservoir setting. It does not imply hydraulic or sedimentary continuity between the pre- and post-impoundment systems.

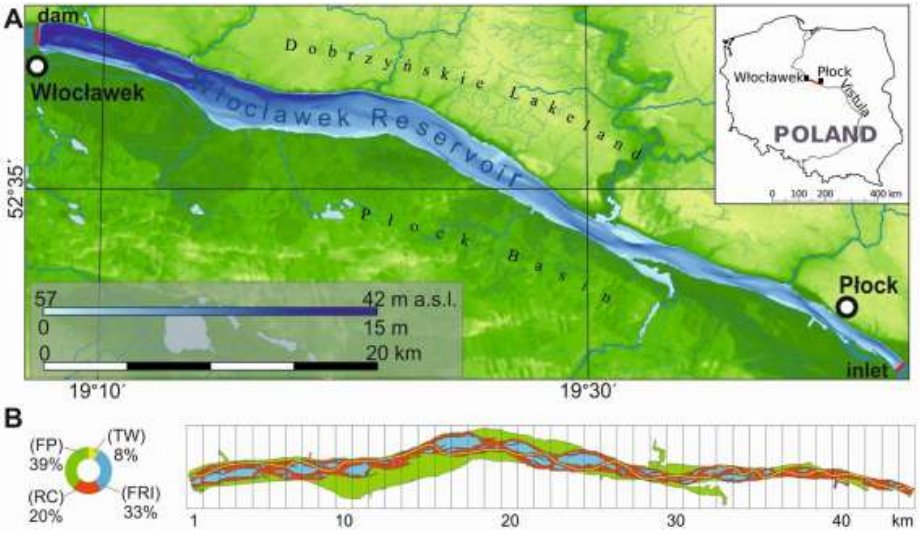


Fig. 1. Study area: (A) location and bathymetry of the Włocławek Reservoir (WR); (B) morphodynamic zones and their areal proportions. Abbreviations: TW — thalweg zone, representing the deepest former primary channel; RC — relict-channel/channel-belt zone, representing secondary and lateral channels; FRI — former island/bar zone; FP — former floodplain zone.

Hydrologically, WR is characterized by relatively stable water-level conditions. The mean inflow in 1971–2023 was 914 $m^3 s^{-1}$ and the mean outflow was 893 $m^3 s^{-1}$. Annual water-level fluctuations in the lower part of the reservoir ranged from 52 to 187 cm, while daily amplitudes on more than 200 days per year were <5 cm (Gierszewski, 2018). The mean residence time in this strongly polymictic reservoir is approximately 5.2 days.

Despite the relatively stable water levels, internal hydromorphological and sedimentary processes remain dynamic. Previous studies indicate that wind-induced mixing may enhance sediment resuspension, especially in shallow areas, whereas inherited morphological features of the former river channel steer throughflow and sediment transport within the reservoir. In the present study, the modelling focuses on the latter component, i.e. the interaction between reservoir throughflow and inherited bed morphology. At the scale of the whole Włocławek Reservoir, only 14% of the reservoir area lies outside the former Vistula channel/corridor (Gierszewski, 2018), confirming the strong imprint of pre-impoundment fluvial morphology on the present reservoir bed. This value should not be directly compared with the zone percentages reported here, which refer to the analysed dam–Płock modelling domain and to a more detailed subdivision of the former channel belt and adjacent floodplain surfaces.

Bedload in the Vistula upstream of WR may constitute up to ~77% of the total sediment load (Babiński, 2005). It is estimated that the reservoir traps nearly 100% of this material and 40–60% of the suspended load (Babiński, 1994; Łajczak, 1999; Gierszewski, 2018). The Vistula is the main source of suspended matter to the reservoir, contributing approximately 96% of the suspended load (Banach, 1994). The long-term mean concentration of total suspended solids (TSS) 20–25 km upstream of the backwater is 28 mg L^{-1}, which is within the typical range for lowland rivers, i.e. 20–100 mg L^{-1} (Meybeck et al., 2003). Upon entering the reservoir, the

https://doi.org/10.5194/egusphere-2026-6675
Preprint. Discussion started: 4 November 2026
© Author(s) 2026. CC BY 4.0 License.

suspended load undergoes qualitative and quantitative changes due to sedimentation and resuspension (Gierszewski, 2018).

The bottom sediments exhibit pronounced longitudinal zonation: sand dominates the riverine and transitional zones, whereas silt and clay prevail in the lacustrine zone. In terms of grain-size composition, silt fractions dominate (67%), followed by sand (25.9%) and clay (7.1%) (Gierszewski, 2018). This longitudinal sedimentary zonation coexists with the inherited morphodynamic zonation analysed in this study.

The coexistence of erosional and depositional sub-environments, resulting from reservoir-bed configuration and the combined action of wind-driven currents and throughflow circulation, favours the formation of dynamically evolving sedimentary structures. This is reflected in the strong spatial variability of sediment-accumulation rates (Bogucka-Szymalska and Magnuszewski, 2007; Gierszewski, 2018; Hachaj et al., 2024). The diverse hydrodynamic and sedimentary conditions in WR make it a suitable natural laboratory for investigating how fluvial memory influences suspended-sediment routing, depositional stability and secondary redistribution in valley-type reservoirs.

2.2 Data sources

2.2.1 Suspended-sediment characteristics at the reservoir inflow

To constrain the particle-tracking simulations with field-based sediment data, we used empirical grain-size data for suspended sediment entering WR. The samples were collected at the Płock road–rail bridge cross-section, located 42 km upstream of the dam, at three sampling points distributed across the channel (Fig. 1A). A detailed description of the suspended-sediment sampling procedures, laboratory analyses and sedimentological results is provided in Hachaj et al. (2024). Below, we summarize only the parameters used as model inputs.

The simulations incorporated measurements from three dates representing contrasting flow conditions: 29 August 2012 (low flow, Q = 411 $m^3 s^{-1}$), 15 July 2013 (medium flow, Q = 852 $m^3 s^{-1}$) and 20 April 2013 (high flow, Q = 2,990 $m^3 s^{-1}$). Mean total suspended solids (TSS) concentrations at the Płock cross-section ranged from 10.3 to 41.2 mg L^{-1} and increased with discharge. These values are consistent with the long-term TSS concentrations observed in the Vistula upstream of WR (Gierszewski, 2018). In all three cases, the highest TSS concentrations occurred in the central part of the cross-section, ranging from 12.8 to 49.7 mg L^{-1}. The suspended load consisted predominantly of a non-volatile fraction (NVSS), with a mean share of 81.5%, similar across all sampling points.

Within the mineral fraction of the suspended load, silt dominated, with a mean share of 93.6%, followed by clay (5.9%) and sand (0.5%). In the high-flow sample, the sand fraction reached up to 3.2%. The mean grain size (Mz) ranged from 0.011 to 0.013 mm, corresponding to medium silt. All samples showed unimodal grain-size distributions, with modes between 0.017 and 0.021 mm, corresponding to coarse silt, poor sorting, and positive to strongly positive skewness.

2.2.2 Hydrological regime of the Vistula upstream of the reservoir

Simulations of flow velocity, suspended-sediment transport and deposition were carried out using hydrological data from the 2012–2013 study period. Mean daily discharges of the Vistula recorded at the Kępa Polska gauging station, located in the backwater reach upstream of the reservoir, were obtained from the open-access databases of the Institute of Meteorology and Water Management – National Research Institute (IMGW-PIB) in Warsaw. Mean daily water levels at the dam were provided by the State Water Holding "Polish Waters" (PGW Wody Polskie).

The hydrological regime of the Vistula during the 2012–2013 study period did not differ substantially from the river's typical multi-annual regime (Gierszewski, 2018). The hydrograph was characterized by distinct spring snowmelt floods and rainfall-driven floods during the warm season (Fig. 2). In winter and late summer–autumn, discharges generally remained within 500–600 $m^3 s^{-1}$, close to the low-flow threshold (Qthr_LF = 552 $m^3 s^{-1}$). Flows below this threshold occurred five times, with a cumulative duration of 248 days. During the longest low-flow phase, from 24 August 2012 to 2 November 2012, the minimum discharge reached 327 $m^3 s^{-1}$.

The spring snowmelt flood of 2012 reached the high-flow threshold (Qthr_HF = 1,630 $m^3 s^{-1}$). Its hydrograph was relatively gentle, with prolonged rising and falling limbs, followed by stabilization at baseflow levels. In spring 2013, the regime became much more variable: from April to May, a series of abrupt high-flow events occurred, peaking above 3,500 $m^3 s^{-1}$, and several further intense events were recorded in summer. The long-term mean discharge (MAD = 914 $m^3 s^{-1}$) was repeatedly exceeded during this period.

Three representative periods were selected for simulating the distribution of flow velocities in WR:
(i) 29 August 2012–9 September 2012 — a phase of relatively stable late-summer low-flow conditions, with discharges from 331 to 411 $m^3 s^{-1}$;
(ii) 15 July 2013–23 July 2013 — a phase of moderate flows, oscillating between 841 and 1,030 $m^3 s^{-1}$, following a series of summer high-flow events with peaks up to approximately 2,800 $m^3 s^{-1}$;
(iii) 20 April 2013–5 May 2013 — the recession phase of the spring flood, with discharges from 1,780 to 2,990 $m^3 s^{-1}$.

https://doi.org/10.5194/egusphere-2026-6675
Preprint. Discussion started: 4 November 2026
© Author(s) 2026. CC BY 4.0 License.

Together, these periods represent a broad range of hydraulic conditions relevant to suspended-sediment routing in WR, from prolonged low-flow conditions to moderate post-flood flows and the recession phase of a spring flood.

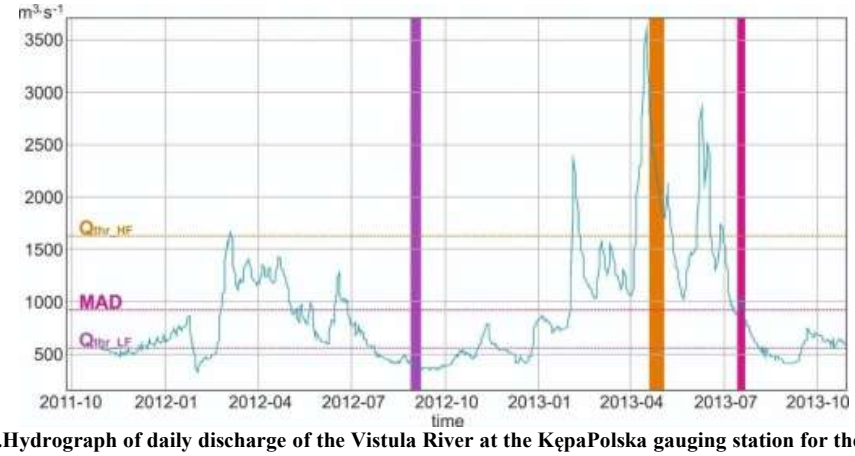


Fig. 2.Hydrograph of daily discharge of the Vistula River at the KępaPolska gauging station for the 2012–2013 study period. Thresholds shown: Qthr_HF — high-flow threshold discharge; MAD — mean annual discharge; Qthr_LF — low-flow threshold discharge. Highlighted periods denote the intervals used for the simulations.

2.2.3 Cartographic and bathymetric reconstruction of morphodynamic zones

To delineate and quantify the morphodynamic zones, we used the most recent reservoir bathymetry together with pre-impoundment topographic maps and aerial photographs. The source material comprised 14 sheets of 1:10,000-scale detailed topographic maps (Head Office of Geodesy and Cartography, GUGiK; 1957–1961), aerial photographs from the National Geodetic and Cartographic Resource (1961–1965), and the 2012 bathymetric survey of the reservoir. These datasets were used to reconstruct the pre-impoundment channel–island–floodplain pattern and to delineate four morphodynamic zones used in the subsequent analyses: thalweg zone (TW), relict-channel/channel-belt zone (RC), former island/bar zone (FRI), and former floodplain zone (FP).

WR bathymetry was measured in September 2012 with a Teledyne ODOM Echotrac E2 single-beam echo sounder (SBES) coupled to a GNSS/GPS receiver. Cross-sections were surveyed at 150 m spacing, and the data were imported into SAGA GIS v.2.3.2 to construct a digital elevation model (DEM) with a 3.0 × 3.0 m resolution (Tutro et al., 2022). Scattered points were interpolated using the multilevel B-spline method of Lee et al. (1997). The resulting bathymetry was then used to prepare the mesh geometry for the 2-D hydrodynamic model.

Archival topographic maps of the Vistula channel were scanned at 600 dpi and georeferenced by a second-order polynomial transformation to the national PUWG “1992” projected coordinate system (EPSG:2180). The scanned aerial photographs were orthorectified in an analogous manner using ground control points (GCPs). For each map and photograph sheet, the following features were digitised: the bankline, defined as the outline of the main channel; the main flow path, represented by a centreline polyline and an associated buffer used to support TW delineation; and channel forms, including river islands and bars digitised as polygons.

The thalweg zone (TW) was delineated along the reconstructed axis of the former main Vistula channel. This axis was derived from the digitised main flow path and adjusted with reference to the position of islands and bars visible on archival maps and aerial photographs. It was then compared with the line connecting the deepest points in bathymetric cross-sections. A representative TW width of approximately 100 m was adopted on the basis of the reconstructed main-flow corridor, the distribution of deepest points in bathymetric cross-sections, and the typical scale of the lower Vistula channel.

The former island/bar zone (FRI) was delineated from the mapped outlines of former islands and sandy bars. Because both former islands and bars represent elevated, relatively lower-energy elements of the pre-impoundment channel belt compared with the main and secondary channels, they were treated together as one inherited morphodynamic unit. The relict-channel/channel-belt zone (RC) was defined as the remaining part of the former active channel belt outside the narrow TW corridor and outside the mapped island/bar polygons. Areas located outside the former active channel belt, but inundated after dam construction, were assigned to the former floodplain zone (FP).

Cartometric analysis involved GIS-based processing and statistical summaries of reconstructed features. The temporal and spatial consistency of the reconstructed morphodynamic template was assessed by comparing maps, aerial photographs and the bathymetric plan. Spatial overlaps between reconstructed features from

https://doi.org/10.5194/egusphere-2026-6675
Preprint. Discussion started: 4 November 2026
© Author(s) 2026. CC BY 4.0 License.



successive datasets were quantified in ArcGIS Pro using overlay and clipping operations. These analyses were used to compare the lengths of coincident main-channel centreline segments and the areas of overlapping island/bar polygons.

The area of each morphodynamic zone was calculated in GIS and expressed as a percentage of the analysed reservoir-bed area. These areal proportions were subsequently used to normalize sediment-deposition data and to calculate zone-specific sedimentation indices.

The resulting zonation provided the spatial framework for comparing modelled velocity fields, particle trajectories, sedimentation efficiency, and resuspension–redeposition patterns.

2.3 Methods for analysing suspended-sediment transport and deposition

2.3.1 Hydrodynamic modelling with AdH

Hydrodynamics were simulated using the Adaptive Hydraulics model (AdH), developed by the U.S. Army Corps of Engineers (Savant and Berger, 2012; Berger et al., 2013). AdH is a two-dimensional (2-D), depth-averaged finite-element model suitable for hydrodynamic simulations in rivers, flow-through lakes, dammed reservoirs, and coastal embayments (Tate et al., 2014; Herrera-Díaz et al., 2017; Liu et al., 2021). It has been successfully applied to several Polish reservoirs, including the WR (Hachaj et al., 2015; Hachaj, 2018; Tutro et al., 2022; Hachaj et al., 2024). The model solves the depth-averaged shallow-water equations for continuity and momentum using the finite-element method and an Eulerian frame of reference (Berger et al., 2013).

$$\frac{\partial v_x}{\partial t} + v_x \frac{\partial v_x}{\partial x} + v_y \frac{\partial v_x}{\partial y} - C_f \cdot v_y + g \frac{\partial \zeta}{\partial x} + g \cdot v_x \frac{\sqrt{v_x^2+v_y^2}}{C^2 \cdot H} - \nu \left(\frac{\partial^2 v_x}{\partial x^2} + \frac{\partial^2 v_x}{\partial y^2}\right) + \frac{1}{\rho_w}\frac{\partial p}{\partial x} = f_x \frac{\partial v_y}{\partial t} + v_x \frac{\partial v_y}{\partial x} + v_y \frac{\partial v_y}{\partial y} - C_f \cdot$$

$$v_x + g \frac{\partial \zeta}{\partial y} + g \cdot v_y \frac{\sqrt{v_x^2+v_y^2}}{C^2 \cdot H} - \nu \left(\frac{\partial^2 v_y}{\partial x^2} + \frac{\partial^2 v_y}{\partial y^2}\right) + \frac{1}{\rho_w}\frac{\partial p}{\partial y} = f_y \qquad (1)$$

where: vx,vy (m s⁻¹) — depth-averaged velocity components; fx,fy (m s⁻²) — specific forcing terms (accelerations) due to wind stress at the free surface and wave forcing; Cf (s⁻¹) — Coriolis parameter; g(m s⁻²) — gravitational acceleration; ζ (m) — water-surface elevation; H(m) — water depth;C(m¹′² s⁻¹) — Chézy roughness coefficient;ν(m² s⁻¹) — kinematic viscosity;p(Pa) — external pressure;ρw (kg m⁻³) — water density.

Model inputs included a bathymetric map of the reservoir bed, water-surface elevation at the outflow boundary, and discharges at all inflow boundaries. Boundary conditions were prescribed as either constant or time-varying, depending on the simulation scenario. The model was initialized from rest, with zero velocity and a horizontal free surface across the computational domain. The main AdH outputs used in this study were two-dimensional, depth-averaged horizontal velocity fields and scalar water-surface elevation (WSE).

The AdH model had previously been calibrated and verified for WR by Tutro et al. (2022), who compared modelled velocities with field measurements for eight distinct total-inflow levels. The model reproduced reservoir hydrodynamics over a wide range of WSE and inflow conditions. All simulations reported here used the calibrated setup from Tutro et al. (2022), including a bed-roughness coefficient of 0.035 and a +10% flow correction at the upstream boundary. Other numerical settings followed the calibrated configuration described in that study. In the present simulations, wind- and wave-related forcing terms were set to zero.

2.3.2. Particle-tracking modelling with PTM

Suspended-sediment transport was simulated using the Particle Tracking Model (PTM; MacDonald et al., 2006).Unlike most Eulerian models that represent sediment as a continuum, PTM employs a Lagrangian, particle-based approach (Bennett, 2006), in which representative particles are transported through previously computed velocity fields. Each representative particle corresponds to a specified mass of real sediment of a given diameter. When a particle deposits at a given location, it represents deposition of that sediment mass in its vicinity. This approach allows both the transported mass and the grain-size distribution (GSD) of deposited material to be tracked.

Particle-transport rates were computed using the Soulsby–van Rijn formulation (van Rijn, 1984; Soulsby, 1997), as implemented in PTM.

$$q_t = As\left(\left(U^2 + \frac{0.018}{c_D}U_w^2\right)^{\frac{1}{2}} - U_{cr}\right)^{2.4} \qquad (2)$$

where: qt(m² s⁻¹) — total sediment transport rate; As(-)— grain-size-dependent coefficient; U(m s⁻¹) — depth-averaged horizontal velocity; Uw (m s⁻¹) — near-bed wave orbital velocity; CD— wave-induced drag coefficient; Ucr(m s⁻¹) — critical flow velocity for incipient motion (and the suspension threshold, where applicable).

The relation accounts for depth-averaged flow velocity, critical velocity for incipient motion, grain-size-dependent transport parameters and, where applicable, near-bed wave orbital velocity. Because surface-wave forcing was neglected in the present simulations, the wave-related term was set to zero.

PTM inputs comprised the reservoir bathymetric map and the WSE and velocity fields generated by AdH. Representative particles were released from an ellipsoidal source zone located in the upstream part of the

https://doi.org/10.5194/egusphere-2026-6675
Preprint. Discussion started: 4 November 2026
© Author(s) 2026. CC BY 4.0 License.

computational domain. Particle density was assumed constant at 2,650 kg m^{-3}, representing mineral sediment. The representative particle diameter can be either fixed or sampled from a normal distribution in phi units, corresponding to a lognormal distribution in millimetres. The fixed-diameter option was previously used for model validation (Hachaj et al., 2024), whereas the distributed-diameter option was used here to represent the observed suspended-sediment events.

It should be emphasized that the present PTM simulations did not include erosion of the natural reservoir bed or exchange with deeper pre-existing bed sediments defined by a vertical grain-size profile. The measured reservoir bathymetry was used as the fixed morphological boundary condition for the hydrodynamic model, whereas the particles introduced into PTM represented the suspended load entering the reservoir during the analysed events. In this framework, primary deposition, resuspension and secondary deposition were distinguished on the basis of the trajectory history of each representative particle. The first settling event was recorded as primary deposition; subsequent re-entrainment of a previously deposited modelled particle was recorded as resuspension; and settling after re-entrainment was recorded as secondary deposition. Thus, the proportions of these categories were not prescribed in advance, but calculated from particle counts, or equivalent particle mass, within each flow scenario and morphodynamic zone.

2.3.3. Model evaluation and simulation scenarios

Calibration and evaluation of the AdH–PTM modelling chain for WR were based on previously published field-data comparisons. The hydrodynamic component was calibrated and verified by Tutro et al. (2022), whereas the PTM component was evaluated in previous applications to WR by Hachaj et al. (2024) and Mączka et al. (2024). In those studies, model outputs were consistent with the observed spatial pattern of bed-sediment grain sizes and with mapped depositional and erosional zones. In the present study, the modelling chain was additionally constrained by measured bathymetry, observed discharge and water-level records, and empirical suspended-sediment grain-size distributions at the inflow cross-section. Therefore, the AdH–PTM framework was used here as an already calibrated and field-evaluated modelling approach, rather than as a newly developed, unverified model.

Although these calibration and evaluation studies were published separately, the simulations analysed here were based on a temporally consistent archival dataset: the 2012 reservoir bathymetry, 2012–2013 hydrological boundary conditions, and suspended-sediment measurements from the same analysed events. The calibrated AdH–PTM setup was therefore applied to reproduce event-scale sediment routing over the measured reservoir morphology, not to simulate the present-day bed configuration or long-term reservoir infilling.

Hydrodynamic simulations were undertaken for three observed flow periods at a normal pool level of WSE = 57.26 m a.s.l.: (i) low flow, lasting 11 days, with discharges from 331 to 411 $m^3 s^{-1}$; (ii) medium flow, lasting 8 days, with discharges from 841 to 1,030 $m^3 s^{-1}$; and (iii) high flow, lasting 15 days, with discharges from 1,780 to 2,990 $m^3 s^{-1}$.

These scenarios represent hydrological throughflow conditions and do not include separate operational variants of dam management, such as controlled drawdown, sediment flushing or bottom-outlet release events. PTM simulations were then performed for the corresponding scenarios using a particle-size distribution matched to the measured suspended-sediment GSDs at the reservoir inflow.

These simulations should therefore be interpreted as representative event-scale simulations rather than steady-state runs based on three isolated discharge values. They were designed to capture the sediment-transport response to contrasting hydrological situations: prolonged low flow, near-mean flow following summer floods, and the recession phase of a spring flood. The main text presents longitudinal profiles and zone-based summaries, whereas spatially explicit, time-dependent animations of the AdH–PTM simulations are available in the associated research dataset (Tutro, 2026).

2.3.4. Representation of suspended-sediment grain-size distributions

When modelling real-world suspended-sediment transport in a Lagrangian framework, reproducing the inflow grain-size distribution is essential. If the particle-size distribution prescribed for the model source matches that measured at the reservoir inflow cross-section, each representative particle can be assigned the same mass of real sediment irrespective of its diameter. This ensures that the modelled particle population represents both the mass and grain-size structure of the suspended load entering the reservoir.

Measured phi-scale grain-size distributions are shown in Fig. 3. They were approximately bell-shaped but exhibit more than one mode; therefore, each distribution was approximated as a finite Gaussian mixture. A two-component mixture was insufficient, whereas a three-component mixture reproduced the measured curves well. Each component was characterised by a mean, standard deviation and weight. Because the three weights sum to 100%, the total number of independent fitting parameters was eight: three means, three standard deviations and two independent weights.

Within the modelled source zone, three sub-sources of representative particles were defined: coarse, medium and fine. Their parameters were tuned to match the measured suspended-sediment GSDs for the three

https://doi.org/10.5194/egusphere-2026-6675
Preprint. Discussion started: 4 November 2026
© Author(s) 2026. CC BY 4.0 License.

analysed events. The modelled source distribution was then obtained as the sum of the three Gaussian components. Random sampling of representative particles from the fitted distributions may produce small fluctuations around the fitted curves, but preserves the overall structure of the measured GSDs.

The measured GSD shows a relatively steep coarse-end tail, reflecting the limited contribution of coarse grains to the suspended load because of their higher settling velocities. The relative deficit of the finest clay-size fraction may reflect the greater tendency of clay particles to flocculate, which can enhance settling relative to individual mineral grains. The measured and modelled grain-size distributions used in the PTM simulations are shown in Fig. 3.

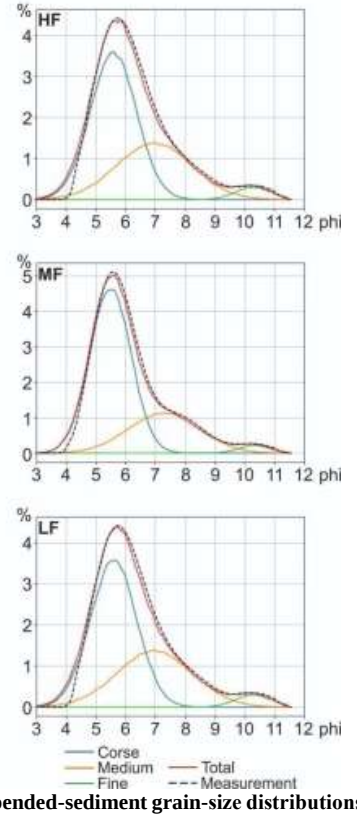


Fig. 3. Measured and modelled suspended-sediment grain-size distributions in the Vistula River at the Plock cross-section for the three analysed events.

2.3.5. Model-derived indicators of sediment retention, stability and redeposition

The three indicators were designed to convert spatially explicit AdH–PTM outputs into interpretable diagnostic metrics of reservoir functioning. They were not intended to replace detailed two-dimensional model fields, but to summarize three complementary aspects of sediment dynamics that are relevant for hydromorphological assessment and sediment management: disproportionate sediment capture, stability of primary deposition, and the contribution of secondary redistribution.

The inherited morphodynamic zones were used to aggregate spatially explicit 2-D model outputs into geomorphologically meaningful units, allowing direct comparison of sedimentation efficiency, depositional stability and redeposition among the thalweg zone (TW), relict-channel/channel-belt zone (RC), former island/bar zone (FRI), and former floodplain zone (FP). All indices were calculated separately for each flow scenario and morphodynamic zone. Only particles released during a given simulation were considered; therefore, the indices describe event-scale sediment dynamics rather than long-term sediment accumulation.

To assess the propensity of individual morphodynamic zones to accumulate suspended sediment, we introduce the Relative Sedimentation Efficiency index (RES):

$$RES = \frac{Z_i}{P_i} : \frac{Z_{tot}}{P_{tot}} = \frac{Z_i \cdot P_{tot}}{Z_{tot} \cdot P_i} \qquad (3)$$

https://doi.org/10.5194/egusphere-2026-6675
Preprint. Discussion started: 4 November 2026
© Author(s) 2026. CC BY 4.0 License.

where: Z_i — is the number, or equivalent mass, of particles remaining deposited in zone (i) at the end of the simulation; P_i — is area of zone i; Z_{tot} — is the total number, or equivalent mass, of particles remaining deposited in the analysed reservoir-bed domain at the end of the simulation; P_{tot} — is the total bed area of the analysed domain.

RES is dimensionless and expresses sediment capture normalized by the areal share of each morphodynamic zone. Values of ($RES_i > 1$) indicate disproportionately high sedimentation efficiency, meaning that a zone captures more sediment than expected from its bed-area share. Values close to 1 indicate proportional sedimentation efficiency, whereas values of ($RES_i < 1$) indicate disproportionately low sediment capture. RES can be calculated from particle counts, mass or volume, provided that the same quantity is used consistently in the numerator and denominator.

To evaluate the influence of resuspension on depositional stability, we used the Sediment-deposition Stability Index (SDI). Based on trajectory history, modelled particles that settled to the bed were assigned to three categories: PDG — primary-deposition particles; SDG — secondary-deposition particles; RG — particles that, after initial deposition, were re-entrained from the bed.

For SDI, only the first deposition event of each particle was considered. $(PDG)_i$ denotes particles whose first deposition occurred in zone (i) and which remained there without subsequent remobilization, whereas (RG_i) denotes particles whose first deposition occurred in zone (i) but which were subsequently re-entrained from that zone. Secondary-deposition particles (SDG_i) were excluded from SDI because this index is intended to measure the stability of primary deposits at the site of first settling.

$$SDI = \frac{(PDG)_i}{(PDG)_i + (RG)_i} \qquad (4)$$

SDI is dimensionless and ranges from 0 to 1. Values close to 1 indicate high stability of primary deposition, whereas values approaching 0 indicate strong post-depositional remobilization. A value of 0.5 represents an approximate balance between retained and remobilized primary deposits. Thus, lower SDI values identify more dynamic depositional environments in which particles are more likely to be re-entrained after initial settling.

To assess the spatial variability in the contribution of secondary deposition to the final depositional pattern, we propose the Redeposition Index (RI). RI highlights areas where deposition is strongly influenced by sediment that had previously been deposited and subsequently resuspended elsewhere or within the same morphodynamic zone. It is defined as the fraction of secondary-deposition particles in the total number of deposited particles remaining in zone (i) at the end of the simulation:

$$RI = \frac{(SDG)_i}{(PDG)_i + (SDG)_i} \qquad (5)$$

where (SDG_i) denotes particles deposited in zone (i) after previous re-entrainment, and (PDG_i) denotes particles deposited in zone (i) without previous resuspension, both counted within the final deposited particle population. RI is dimensionless and ranges from 0 to 1. Values close to 0 indicate dominance of primary deposition, whereas values approaching 1 indicate a high contribution of redeposited material and therefore active secondary sediment redistribution.

The proposed indices provide a quantitative link between the two-dimensional particle-tracking outputs and the inherited morphodynamic structure of the reservoir bed. RES measures the relative efficiency of sediment capture by individual legacy zones, SDI evaluates the stability of primary deposition, and RI quantifies the contribution of redeposition to the sedimentary pattern. Together, these indices allow the spatially distributed model outputs to be interpreted in terms of fluvial-memory-controlled sediment dynamics.

Because all three indices are dimensionless and can be calculated from particle counts, mass or volume, they may be adapted to other Lagrangian or Eulerian modelling frameworks, provided that input and output quantities are used consistently. Their diagnostic meaning and potential relevance for reservoir assessment and sediment management are summarized in Table 2. This structure follows general indicator-development principles, according to which indicators should have a clear conceptual basis, a reproducible calculation procedure, sensitivity to relevant system variability, and direct interpretability for assessment or management decisions (Kurtz et al., 2001; Dale and Beyeler, 2001).

Table 2. Diagnostic meaning and potential management relevance of the proposed sediment-dynamics indicators.

Indicator	Diagnostic meaning	High values indicate	Low values indicate	Potential use
RES — Relative Sedimentation Efficiency	Relative sediment-capture efficiency normalized by the areal share of a morphodynamic zone	Disproportionately high sediment accumulation; sediment-capture hotspot	Low sediment-capture efficiency relative to zone area	Identification of depositional hotspots; prioritization of monitoring and sediment sampling

https://doi.org/10.5194/egusphere-2026-6675
Preprint. Discussion started: 4 November 2026
© Author(s) 2026. CC BY 4.0 License.

SDI — Sediment-deposition Stability Index	Stability of primary deposition after initial settling	Stable primary deposits; low post-depositional remobilization	Low stability of primary deposition; high post-depositional remobilization	Assessment of depositional stability; identification of areas susceptible to reworking
RI — Redeposition Index	Contribution of secondary deposition to the final deposited material	High contribution of redeposited material; active secondary sediment redistribution	Dominance of primary deposition; limited secondary redistribution	Identification of resuspension–redeposition zones; support for sediment-management planning

3. Results

3.1. Morphodynamic zonation of the reservoir bed

The comparison of the present reservoir bathymetry with the reconstructed pre-impoundment morphology shows that the former Vistula channel–island–floodplain template remains clearly expressed in the reservoir-bed structure (Fig. 1B). This preserved morphology is consistent with earlier observations that the former Vistula channel remains a major structural element of the Włocławek Reservoir bed and continues to influence its hydromorphological functioning (Gierszewski, 2018; Hachaj et al., 2024). The reservoir is therefore not a geomorphologically uniform basin, but a submerged fluvial corridor in which the inherited channel–island–floodplain pattern defines distinct morphodynamic units.

This zonation is based on the 2012 bathymetry and reconstructed pre-impoundment morphology; it is not intended to quantify temporal changes in mean bed elevation or bed slope since impoundment. Instead, the 2012 bathymetry is used as the measured morphological boundary condition for the hydrodynamic and particle-tracking simulations.

Four morphodynamic zones were distinguished. The thalweg zone (TW) forms a narrow, continuous corridor following the deepest part of the former main Vistula channel. Although it occupies only 8% of the analysed reservoir-bed area, it represents the principal inherited flow-routing axis. The relict-channel/channel-belt zone (RC), occupying 20% of the analysed bed area, comprises the broader belt of former main and secondary channels surrounding or branching from the thalweg corridor. Together, TW and RC represent the preserved channel framework of the pre-impoundment Vistula.

Within the analysed dam–Płock reach, the former island/bar zone (FRI) occupies 33% of the modelled reservoir-bed area and consists of submerged former islands and bars embedded within the former Vistula channel belt. This zone is spatially discontinuous and bathymetrically heterogeneous, forming local topographic highs and morphological settings favourable to flow deceleration and sediment deposition. The former floodplain zone (FP) is the largest unit within the analysed reach, covering 39% of the modelled bed area. It corresponds to inundated floodplain surfaces located outside the former active channel belt and forms the main shallow, lower-energy marginal domain.

The areal structure of the reservoir bed shows that the inherited morphology is not limited to a narrow remnant thalweg. Instead, the reservoir retains a laterally structured channel–island–floodplain template, with flow-conducting elements, former island/bar surfaces and marginal floodplain areas arranged across the reservoir width. This preserved spatial organization provides the geomorphic expression of fluvial memory and forms the basis for the subsequent analyses of velocity distribution, suspended-sediment deposition, resuspension, and redeposition.

3.2. Hydrodynamic characteristics of the reservoir

Reservoir hydrodynamics were analyzed for three characteristic Vistula flow events: an 11-day late-summer low-flow period, 29 August–9 September 2012 (331–411 $m^3 s^{-1}$); moderate summer flows following a series of floods, 15–23 July 2013 (841–1,030 $m^3 s^{-1}$); and the recession phase of the spring flood, 20 April–5 May 2013 (1,780–2,990 $m^3 s^{-1}$). Results are presented as: (i) velocity box plots for cross-sections spaced every 1 km from the dam upstream; and (ii) velocity ranks by morphodynamic zone (Fig. 4). Corresponding spatially explicit, time-dependent animations illustrating particle transport, deposition, resuspension, and redeposition under the three flow scenarios are available in the associated research dataset (Tutro, 2026).

https://doi.org/10.5194/egusphere-2026-6675
Preprint. Discussion started: 4 November 2026
© Author(s) 2026. CC BY 4.0 License.

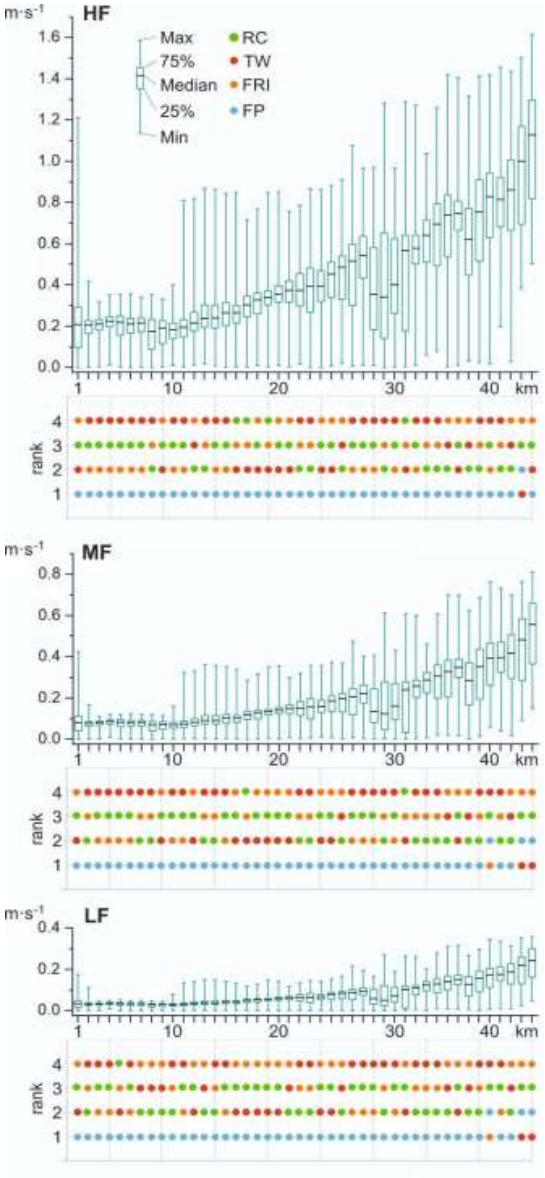


Fig. 4. Spatial distribution of flow velocity in WR under high-flow (HF), medium-flow (MF) and low-flow (LF) conditions: longitudinal profile of velocity (m•s⁻¹) with distance (km) increasing upstream from the dam; and velocity ranks by morphodynamic zone, computed at each reservoir kilometer, from lowest (1) to highest (4).

The rank plots in Fig. 4 show the relative ordering of morphodynamic zones according to flow velocity at each reservoir kilometre, rather than absolute velocity magnitudes. Rank 4 denotes the highest-velocity zone and rank 1 the lowest-velocity zone within a given kilometre segment. Therefore, a nearly straight rank line does not indicate spatially uniform flow. Rather, it indicates that the same inherited morphological unit tends to occupy a similar relative hydraulic position along the reservoir. The persistence of high ranks in TW and RC, and lower ranks in FRI and FP, shows that the former channel belt continues to organize the velocity field under all analysed flow conditions.

https://doi.org/10.5194/egusphere-2026-6675
Preprint. Discussion started: 4 November 2026
© Author(s) 2026. CC BY 4.0 License.

Differences among the LF, MF and HF scenarios are expressed mainly in the absolute velocity values, the lateral extent of the high-velocity core, and the degree of hydraulic connectivity between the thalweg, relict-channel/channel-belt, island/bar and floodplain zones. The two-dimensional AdH velocity fields show that this pattern is not expressed as a uniform longitudinal gradient, but as a laterally differentiated flow structure. The high-velocity corridor remains spatially coherent along the former thalweg, whereas lower-velocity patches occur in the lee of former islands and over shallow marginal surfaces. These patches are most extensive during low-flow conditions and become progressively reduced and more hydraulically connected to the main flow under medium- and high-flow conditions.

Along the longitudinal profile, three reaches stand out: (i) a near-dam reach with relatively high median velocities, associated with outlet structures and the hydropower plant; (ii) a middle reach with the largest share of low-velocity areas, especially during low flows; and (iii) an upper reach where floods generate the broadest swath of high velocities associated with river inflow.

As discharge increases, the high-velocity core widens, low-velocity areas contract, and cross-channel velocity contrasts weaken. During low flows, the velocity field is strongly heterogeneous: a narrow, well-defined core adjoins extensive low-velocity zones. Under medium-flow conditions, this contrast diminishes, and previously weak-throughflow areas shift toward throughflow conditions. During high flows, the velocity field becomes more laterally connected; low-velocity zones are reduced and persist mainly as local flow shadows in the lee of former islands and headlands, and within zones of cross-sectional expansion downstream of constrictions.

Regardless of hydrologic conditions, TW and RC attain the highest velocity ranks, generally 3–4, whereas FRI and FP retain low ranks, generally 1–2, during low and medium flows. During high flows, parts of the former island/bar and floodplain zones become hydraulically activated, shifting to intermediate ranks, generally 2–3, owing to increased connectivity with the main flow corridor (Fig. 4).

In summary, the velocity field retains a persistent imprint of the inherited channel–island–floodplain template: higher velocities are concentrated along the former thalweg and relict-channel/channel-belt zones, whereas lower-energy conditions persist over former island/bar and floodplain zones. The areal extent of high- and low-velocity zones, as well as the magnitude of cross-sectional contrasts, are discharge-controlled, with the clearest expression in the middle and upper reaches of the reservoir.

3.3. Suspended-sediment transport and deposition in the reservoir

3.3.1. Flow-dependent patterns of suspended-sediment deposition

The simulations indicated strong flow-dependent differences in suspended-sediment retention within the reservoir. During the high-flow scenario (1,780–2,990 $m^3 s^{-1}$), 66% of the released suspended-sediment particles, or equivalent sediment mass, remained deposited within the model domain. Under medium-flow conditions (841–1,030 $m^3 s^{-1}$), the modelled retention increased to 73%, whereas at the end of the low-flow scenario (331–411 $m^3 s^{-1}$), it reached 94%. The remaining particles were transported through the reservoir and exported downstream.

During high flow, deposition was less continuous and more spatially dispersed. Sedimentation occurred primarily in the lower part of the reservoir, from the dam to approximately 15 km upstream, and across former floodplain surfaces. Kilometre-scale gaps in deposition continuity occurred along the reservoir, whereas in the upper reach suspended-sediment deposition was weak. Deposits formed during high flow were dominated mainly by medium- and coarse-silt fractions (Fig. 5).

Under medium-flow conditions, suspended sediment was deposited along nearly the entire length of the reservoir, except in the upper segment of the thalweg zone (TW), where throughflow dominated. Across all morphodynamic zones, the highest deposition intensity occurred in the middle reach of the reservoir. Deposits were dominated by fine-silt fractions, with a minor sand component within the relict-channel/channel-belt zone (RC) and, to a lesser degree, on former island/bar surfaces (FRI) located in the upper reach of the reservoir (Fig. 5).

Under low-flow conditions, deposition extended along the full length of the reservoir and occurred in all morphodynamic zones. The greatest deposition intensity was found within the relict-channel/channel-belt zone (RC) and on former island/bar surfaces (FRI), especially in the upper reach of the reservoir, between approximately 30 and 40 km upstream from the dam. In this segment, sand and medium- to coarse-silt fractions prevailed, whereas the lower reach was dominated by fine-silt and clay-sized fractions (Fig. 5).

Figures 5–9 summarize the spatially explicit PTM outputs in relation to reservoir distance and inherited morphodynamic zones. Because PTM is a Lagrangian particle-tracking model, these outputs represent particle pathways and event-based patterns of deposition, resuspension, and redeposition rather than continuous Eulerian suspended-sediment concentration fields. Spatially explicit, time-dependent animations of the PTM simulations are available in the associated research dataset (Tutro, 2026), whereas the main-text figures synthesize cumulative patterns within the TW, RC, FRI, and FP zones.

The deposition fields indicate that sediment accumulation is spatially patchy rather than laterally uniform. Depositional patches occur preferentially along the margins of the former channel belt, around former islands and bars, and in local low-velocity zones adjacent to the main transport corridor. This pattern is most pronounced under

https://doi.org/10.5194/egusphere-2026-6675
Preprint. Discussion started: 4 November 2026
© Author(s) 2026. CC BY 4.0 License.

low- and medium-flow conditions, whereas during high flows the depositional field becomes more dispersed and shifts toward hydraulically connected channel-belt and downstream areas.

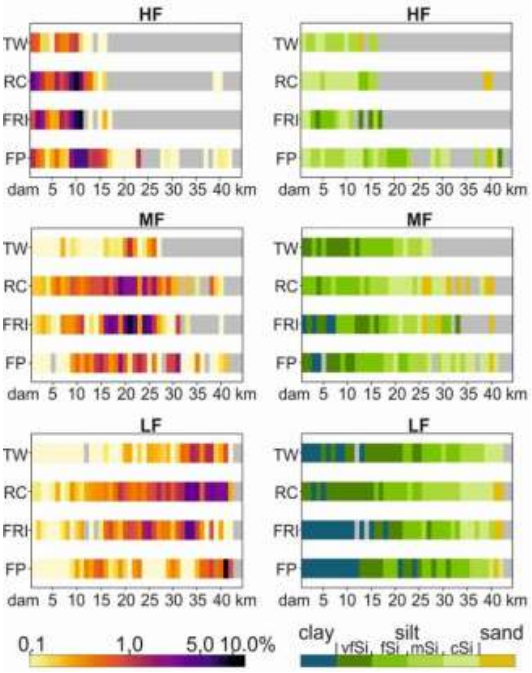


Fig. 5. Longitudinal and zone-based synthesis of suspended-sediment deposition under high-flow (HF), medium-flow (MF), and low-flow (LF) conditions. The figure summarizes the intensity and grain-size structure of deposited particles along the reservoir profile and within the principal inherited morphodynamic zones: TW—thalweg zone; RC—relict-channel/channel-belt zone; FRI—former island/bar zone; and FP—former floodplain zone. Spatially explicit, time-dependent animations of particle transport and deposition are available in the associated research dataset (Tutro, 2026). Grain-size abbreviations: vfSi — very fine silt; fSi — fine silt; mSi — medium silt; cSi — coarse silt.

3.3.2. Relative sedimentation efficiency of inherited morphodynamic zones

Following the diagnostic framework summarized in Table 2, the capacity of each morphodynamic zone to trap suspended sediment was assessed using the Relative Sedimentation Efficiency (RES) index. Model simulations indicate that the thalweg zone (TW) and former-island/bar zone (FRI) exhibited the highest relative sedimentation efficiency, whereas the former floodplain zone (FP) consistently showed the lowest efficiency relative to its areal extent (Table 3).

In the thalweg zone (TW), RES was highest under low-flow conditions and remained high during high flow. The very high low-flow value reflects the concentration of deposition within a narrow inherited flow-routing corridor. In contrast, within the former island/bar zone (FRI), the most favourable conditions for sediment capture occurred under medium-flow conditions, which corresponded to near-mean discharge. The relict-channel/channel-belt zone (RC) showed intermediate to low RES values in all scenarios, whereas FP showed low RES values under low- and medium-flow conditions and a slightly higher value during high flow.

Table 3. Variation in Relative Sedimentation Efficiency (RES) across morphodynamic zones, normalized by each zone's areal share of the analysed reservoir-bed domain, for the three hydrological scenarios: high flow (HF), medium flow (MF) and low flow (LF).

Scenario	Former floodplain zone (FP)	Former island/bar zone (FRI)	Relict-channel/channel-belt zone (RC)	Thalweg zone (TW)
HF	0.46	1.86	0.82	2.29

https://doi.org/10.5194/egusphere-2026-6675
Preprint. Discussion started: 4 November 2026
© Author(s) 2026. CC BY 4.0 License.

MF	0.27	2.63	0.65	1.94
LF	0.28	1.39	0.89	4.10

The consistently high RES values in TW and FRI show that the preserved former thalweg and former island/bar surfaces continue to condition present-day sediment-capture patterns. From an indicator perspective, these zones can be interpreted as sediment-capture hotspots, whereas FP represents a low-efficiency accumulation domain relative to its areal extent.

However, high RES in TW does not mean that the thalweg is the largest absolute sediment sink. Because RES is normalized by areal share, it indicates high deposition density relative to the small area occupied by the thalweg zone. TW therefore remains primarily a transport corridor, but local deposition during low-flow conditions, flow recession and in near-thalweg low-velocity settings produces high areal-normalized sediment-capture efficiency.This distinction is not evident from absolute sediment volumes alone, because they do not account for differences in zone area. RES thus provides a normalized measure of sediment-retention efficiency that is directly comparable among morphodynamic zones.

3.3.3. Depositional stability and secondary redistribution

Depending on hydrodynamic conditions, suspended particles entering the reservoir may pass through the reservoir, settle on the bed, or, after settling, be resuspended and redeposited elsewhere. Particles that remain in place after their first settling are termed primary-deposition particles (PDG), whereas particles that are remobilized after initial deposition and settle again are termed secondary-deposition particles (SDG). Redeposition is therefore interpreted here as the event-scale redistribution of previously deposited modelled particles during changing hydraulic conditions.

The simulations showed that part of the material deposited during variable-flow phases was reactivated, transported and redeposited in other parts of the reservoir. Analysis of suspended-sediment transport and deposition in the Włocławek Reservoir under high-, medium- and low-flow conditions allowed us to: (i) identify areas of primary deposition; (ii) locate zones where deposited particles were first remobilized; and (iii) estimate the contribution of secondary-deposition particles to the final deposited material.

The deposition pattern did not vary monotonically along the reservoir, but depended on both flow regime and inherited morphodynamic zones (Fig. 6). During high flows (HF), primary deposition was spatially restricted, whereas particles remobilized after initial deposition retained high depositional potential, particularly in the downstream, near-dam reach and within the thalweg zone (TW) and relict-channel/channel-belt zone (RC) (Fig. 6B). Within the former floodplain zone (FP), primary deposition was local and discontinuous, whereas secondary-deposition particles formed more extensive bands, although the overall deposition efficiency of FP remained low.

Under medium- and low-flow conditions (MF and LF), deposition of primary suspended sediment was generally more pronounced than secondary deposition. Under MF, primary and secondary depositional patches formed a spatial mosaic, especially within the RC and former island/bar zone (FRI). Under LF, primary deposition dominated over most of the reservoir, while secondary deposition was more restricted and concentrated mainly downstream of local remobilization zones.

Grain size further differentiated primary and secondary deposits (Fig. 6). Deposits derived from primary suspension were generally finer and showed sharper along-profile shifts in grain size. In contrast, secondary-deposition particles covered a broader grain-size spectrum, including coarse silts and sands, especially under HF and locally in the upstream part of the reservoir. Secondary deposits also displayed more gradual textural transitions along the reservoir profile.

https://doi.org/10.5194/egusphere-2026-6675
Preprint. Discussion started: 4 November 2026
© Author(s) 2026. CC BY 4.0 License.

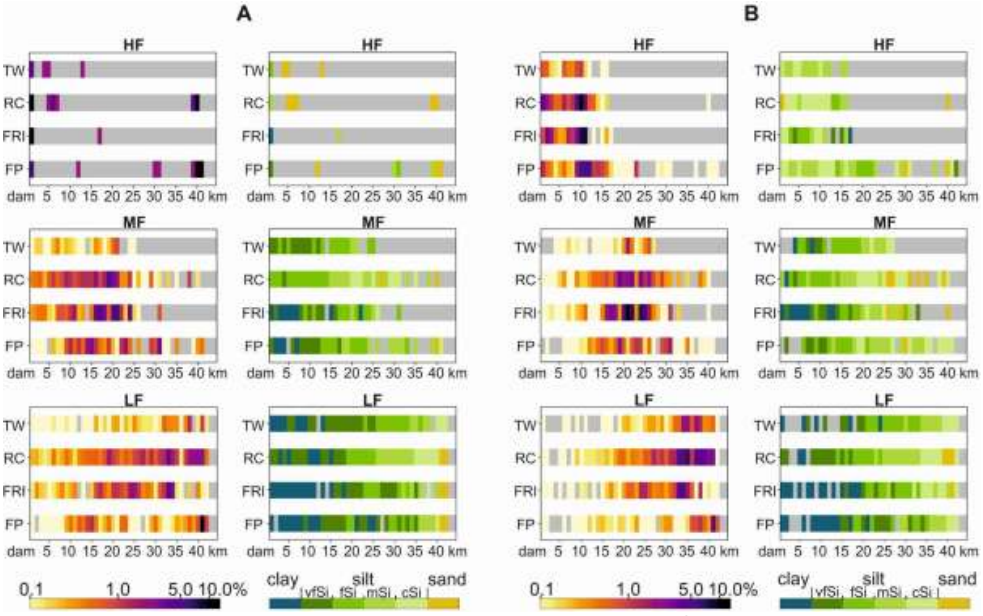


Fig. 6. Longitudinal variability in sedimentation intensity and grain size of (A) primary and (B) secondary suspended-sediment deposition along the reservoir under high-flow (HF), medium-flow (MF), and low-flow (LF) conditions, with the main inherited morphodynamic zones indicated: TW — thalweg zone; RC — relict-channel/channel-belt zone; FRI — former island/bar zone; FP — former floodplain zone. Grain-size abbreviations: vfSi — very fine silt; fSi — fine silt; mSi — medium silt; cSi — coarse silt.

Model simulations identified the locations of first resuspension of previously deposited particles and the corresponding grain-size classes (Fig. 7). During high flows, remobilization occurs along nearly the entire reservoir, with a maximum in the 10–25 km reach upstream of the dam. The highest resuspension intensity occurred mainly within the former island/bar and relict-channel/channel-belt zones (FRI and RC), whereas FP showed weaker remobilization and TW exhibited the lowest values under this scenario. Resuspension during HF involved mainly sand particles, especially within RC, although coarse silts were also entrained in other zones.

https://doi.org/10.5194/egusphere-2026-6675
Preprint. Discussion started: 4 November 2026
© Author(s) 2026. CC BY 4.0 License.

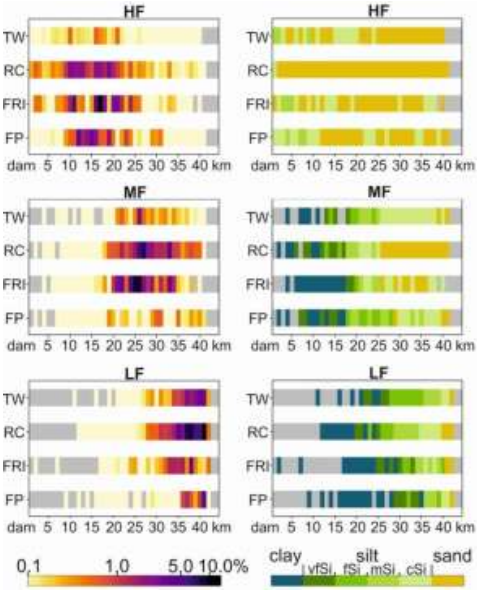


Fig. 7. Spatial pattern of first-resuspension sites of previously deposited primary suspended-sediment particles and their grain-size classes under high-flow (HF), medium-flow (MF) and low-flow (LF) conditions. Grain-size abbreviations: vfSi — very fine silt; fSi — fine silt; mSi — medium silt; cSi — coarse silt.

Under medium-flow conditions, the resuspension maximum shifted upstream, mainly to the 20–40 km reach, and remained concentrated in FRI and RC. Suspended-load transit dominated in TW, where the share of remobilized particles was lower. In the upper part of the reservoir, sands and coarse silts were preferentially entrained, whereas closer to the dam, finer silt and clay-sized particles were more frequently remobilized, including in areas associated with former islands.

Under low-flow conditions, first resuspension was confined mainly to the upper part of the study reach, approximately 25–40 km upstream of the dam. Entrainment was greatest within the former channel belt, but contrasts among morphodynamic zones were smaller than under MF and HF. A downstream fining of remobilized particles was evident: sands dominated in the upstream part of the reach, giving way downstream to coarse and then fine silts, with sporadic clay-sized particles.

The two-dimensional distribution of first-resuspension locations further indicates that remobilization was concentrated along hydraulically active parts of the former channel belt rather than being evenly distributed over the reservoir bed. During high flows, these zones expanded laterally and became connected across larger parts of the reservoir, whereas under low-flow conditions they remained confined mainly to upper and central channel-belt areas.

The influence of resuspension on sedimentation, expressed by the Sediment-deposition Stability Index (SDI), varied systematically with flow conditions (Fig. 8A). During HF, low SDI values (<0.5) dominated in the lower reservoir, especially within the former channel belt, indicating widespread post-depositional remobilization. Under this regime, areas with SDI values clearly above 0.5 were absent or very limited, showing that primary deposits were generally unstable during high-flow conditions.

Under MF, unstable primary deposits shifted upstream and occurred mainly within the former channel-belt zones, with local instability also in TW and FP. This indicates that near-mean discharge conditions following summer floods were sufficient to remobilize part of the previously deposited material, especially in hydraulically connected zones. Under LF, sedimentation was generally more stable; low SDI values occurred only locally, mainly in short upper-reservoir reaches and selected TW segments. Thus, SDI shows that depositional stability increased as flow energy decreased, although local remobilization could still occur in confined, hydraulically active parts of the inherited channel system.

https://doi.org/10.5194/egusphere-2026-6675
Preprint. Discussion started: 4 November 2026
© Author(s) 2026. CC BY 4.0 License.

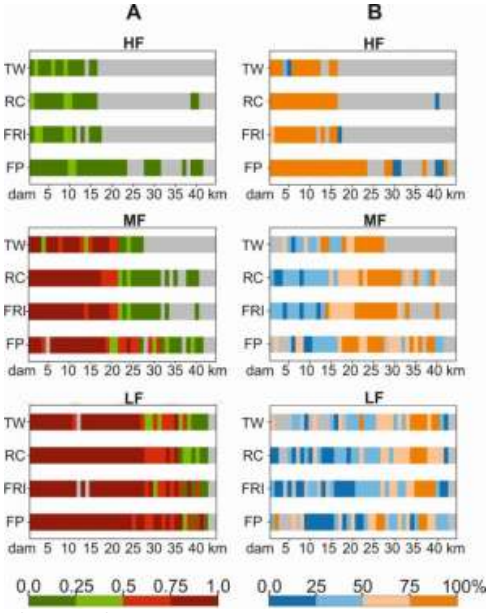
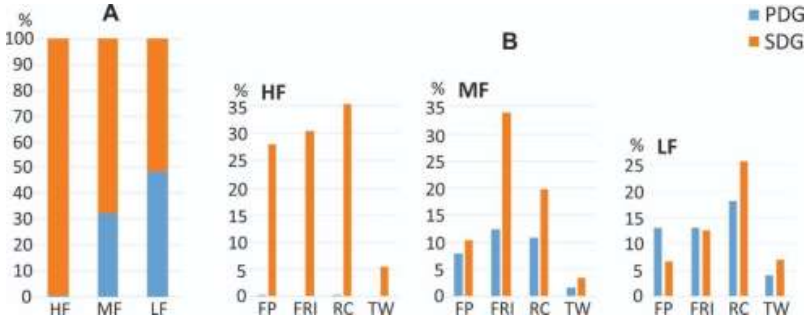


Fig. 8. Assessment of the influence of resuspension on suspended-sediment deposition in the Wloclawek Reservoir (WR) based on (A) the Sediment-deposition Stability Index (SDI), and (B) spatial variability in the contribution of redeposited particles to the total number of deposited particles, expressed by the Redeposition Index (RI).

The spatial contribution of redeposited particles, expressed by the Redeposition Index (RI), also showed a clear flow-regime dependence (Fig. 8B). Under HF, secondary-deposition particles dominated throughout much of the reservoir profile, with high RI values indicating vigorous transport, frequent resuspension and repeated deposition. Under MF, RI revealed a more heterogeneous pattern: redeposition prevailed mainly in the central reach, especially within RC and FRI, whereas segments with a higher share of primary deposition occurred mainly in TW and FP. Under LF, primary-deposition particles dominated, particularly in FP, FRI and RC, and low RI values indicated limited remobilization of previously deposited material.

The two-dimensional redeposition fields further show that secondary deposition formed discontinuous bands and patches downstream of resuspension zones, especially near former islands and along the margins of the inherited channel belt. This pattern indicates that redeposition was controlled not only by longitudinal distance from the dam or inflow, but also by the lateral structure of the preserved pre-impoundment morphology.

The percentage contribution of primary- and secondary-deposition particles confirms the contrast between flow scenarios (Fig. 9). Redeposition dominated under HF, formed a spatial mosaic under MF, and was weakest under LF, when primary deposition prevailed mainly in FP, FRI and parts of RC. The former channel belt and island/bar zones therefore influenced not only primary sediment capture, but also the redistribution of material during resuspension–redeposition cycles.



https://doi.org/10.5194/egusphere-2026-6675
Preprint. Discussion started: 4 November 2026
© Author(s) 2026. CC BY 4.0 License.

Fig. 9. Percentage contribution of primary-deposition particles (PDG) and secondary-deposition particles (SDG) in the sediments of the Włocławek Reservoir: (A) whole-reservoir pattern and (B) individual morphodynamic zones under high-flow (HF), medium-flow (MF) and low-flow (LF) conditions.

Consistent with the diagnostic framework summarized in Table 2, SDI and RI distinguish zones of primary depositional stability from zones where repeated remobilization and secondary deposition dominate the sedimentary pattern. They therefore provide complementary indicators of sediment persistence and sediment mobility within the reservoir bed, showing that fluvial memory controls not only where suspended sediment is initially captured, but also where it is subsequently reworked and redeposited.

4. Discussion

4.1. Fluvial memory as a control on suspended-sediment routing and deposition

The central contribution of this study is conceptual and diagnostic rather than numerical. Established AdH–PTM tools are used to quantify a geomorphological factor that is rarely treated separately in reservoir-sedimentation studies: the persistence of pre-impoundment fluvial morphology as a control on suspended-sediment routing. By combining AdH–PTM modelling with the Relative Sedimentation Efficiency (RES), Sediment-deposition Stability Index (SDI) and Redeposition Index (RI), we translate spatially explicit sediment-transport simulations into process-based indicators of sediment-capture efficiency, depositional stability and secondary redistribution. The results show that deposition, resuspension and redeposition in the Włocławek Reservoir are not controlled solely by present discharge, residence time or longitudinal reservoir geometry, but remain strongly conditioned by the preserved Vistula channel–island–floodplain template.

Earlier applications of the modeling framework showed that the submerged pre-impoundment channel, aligned with the former thalweg (TW), retains a transport function, whereas fine fractions accumulate preferentially in lower-velocity distal and marginal zones of the reservoir (Hachaj et al., 2024). The present study refines this interpretation by showing that spatial variability in hydrodynamics and suspended-sediment deposition is strongly organized by the inherited channel–floodplain morphology. The highest velocity ranks coincide with the former thalweg over most of the reservoir length, while high RES values occur not only in thalweg (TW) but also over former island/bar surfaces (FRI). Such patterns are consistent with the broader concept of fluvial legacy effects, according to which antecedent landforms and sediment-routing structures continue to modulate present-day flow fields and sedimentation patterns (Wohl, 2015, 2019; Buffington and Montgomery, 2022; Sidorchuk, 2003). Similar references to pre-dam morphology appear in studies of reservoir infilling and reservoir-bed evolution (Venteris et al., 2014; Juracek, 2015; Sedláček et al., 2022; Keith et al., 2024; Stauch et al., 2024), indicating that inherited valley-floor morphology may also be relevant for interpreting long-term morphological stability in impounded river systems.

The mechanism by which fluvial memory controls suspended-sediment movement can be summarized as a sequence of linked effects. First, the submerged pre-impoundment morphology creates persistent bathymetric contrasts between the former thalweg, channel belt, island/bar surfaces, and marginal floodplain. Second, these contrasts structure the velocity field by concentrating throughflow along the former thalweg and by generating low-velocity zones and hydraulic shadows around former islands and bars. Third, this hydraulic pattern determines particle trajectories, sedimentation efficiency, and the probability of resuspension and redeposition. Thus, the modelled sediment movement should not be interpreted as a generic reservoir response, but as a response conditioned by the inherited channel–island–floodplain template of the Vistula valley.

The study therefore does not attempt to separate morphological legacy and hydraulic forcing as fully independent controls. In a valley-type reservoir, these factors are physically coupled: inherited bed morphology structures the velocity field, and the resulting hydrodynamics determine particle pathways and depositional behaviour. The LF, MF and HF scenarios were used to test whether this morphology-conditioned pattern persists under contrasting hydraulic forcing. The results indicate that it does, although the spatial extent and intensity of deposition, resuspension and redeposition vary systematically with flow conditions.

This mechanism may also operate in other valley-type reservoirs, especially those with short residence times and well-preserved pre-impoundment channel morphology. However, its strength will depend on the degree to which the original fluvial relief remains preserved and on the extent to which throughflow continues to follow inherited channel pathways. The Włocławek Reservoir is therefore treated here as a representative case of a through-flow reservoir in which sediment routing is conditioned by inherited fluvial morphology rather than by reservoir-scale geometry alone.

The comparison made in this study is not a direct comparison between measured pre- and post-impoundment sedimentation rates. Such a comparison is not possible because spatially distributed observations of suspended-sediment deposition before reservoir creation are unavailable. Instead, the comparison concerns the spatial logic of sediment routing. The pre-impoundment Vistula was a sandy-bed multi-channel system in which the thalweg and secondary channels acted as preferential transport corridors, while island margins, bar lees and floodplain surfaces formed lower-energy depositional environments. The modelled reservoir pattern reproduces

https://doi.org/10.5194/egusphere-2026-6675
Preprint. Discussion started: 4 November 2026
© Author(s) 2026. CC BY 4.0 License.

this spatial organization under altered hydraulic boundary conditions: the former channel belt still routes sediment, former islands and bars act as morphological anchors generating local deposition and redeposition zones, and marginal surfaces function as lower-energy sinks for fine material. Comparable observations from the dam-regulated Dnieper River downstream of the Kaniv HPP show that islands and interchannel forms may strongly influence flow conditions, sediment accumulation, and the redistribution of alluvia in sand-bed multi-channel systems affected by dam operation (Szmanda et al., 2021; Bortnyk et al., 2026). In this sense, fluvial memory denotes the persistence of a sediment-routing template inherited from the pre-dam river, not the preservation of identical sedimentation rates or facies. More than 50 years after impoundment, this inherited channel–island–floodplain template continues to organize the contemporary velocity field, particle pathways, depositional hotspots, and zones of resuspension and redeposition.

Empirical sediment data from previous studies provide an important reference for evaluating the modelled deposition patterns. Earlier investigations of the Włocławek Reservoir documented pronounced bottom-sediment zonation, with sand-dominated deposits in the riverine and transitional zones and silt- and clay-rich deposits in lower-energy lacustrine and marginal areas. They also showed strong spatial variability in sediment thickness and accumulation rates, reflecting the coexistence of transport, erosion, deposition, and redeposition sub-environments (Gierszewski, 2018; Hachaj et al., 2024). These empirical observations are consistent with the model results, which indicate preferential suspended-sediment routing along the former channel belt and enhanced accumulation in low-velocity zones associated with former islands, bars, and marginal surfaces. The previously published sedimentological evidence therefore provides independent support for the model-based interpretation of sediment-routing and accumulation patterns.

4.2. Hydrodynamic mechanisms: morphological anchors, connectivity, resuspension and redeposition

The observed depositional pattern can be explained by the interaction between inherited morphology, flow concentration, lateral hydraulic connectivity, and repeated settling–resuspension–redeposition cycles. These mechanisms determine why some inherited zones act mainly as transport corridors, whereas others function as preferential accumulation or redistribution areas.

The role of morphological anchors — including channel constrictions, relict thalwegs and stable island/bar forms — in shaping sediment accumulation in short-residence-time reservoirs has been emphasized in previous studies (Venteris et al., 2014; Sedláček et al., 2016, 2022). The present results refine this interpretation by showing that high RES values in TW and FRI reflect two complementary mechanisms. In TW, high suspended-sediment fluxes are concentrated within a narrow inherited transport corridor, so even limited deposition produces high relative efficiency after areal normalization. In FRI, former island and bar surfaces generate local deceleration, hydraulic-lee effects and exchange zones along the margin of the main current, favouring preferential settling and repeated redeposition. In broader RC and FP zones, weaker exchange with the main current and larger areal extent reduce RES after normalization, even where the absolute volume of stored sediment may be substantial.

The HF, MF and LF scenarios allow shifts in hydraulic connectivity between the high-velocity core and lateral zones to be interpreted. Under low-flow conditions, the high-velocity core is narrow and sharply separated from extensive low-velocity or weak-throughflow zones. Under medium-flow conditions, this contrast weakens and some previously weakly connected areas shift toward throughflow conditions. During high-flow events, the velocity field becomes more laterally connected and low-velocity zones are reduced, persisting mainly as local hydraulic lees along former islands and headlands or in deceleration zones downstream of constrictions. Consequently, suspended sediment is supplied more effectively to areas that are poorly connected under low-flow conditions, and deposition becomes more spatially dispersed. These observations are consistent with concepts of lateral and longitudinal connectivity in river–valley systems, in which episodic increases in connectivity during floods limit the long-term isolation of lateral zones (Amoros and Roux, 1988; Pringle, 2001). Differences in suspended-sediment capture efficiency between HF and LF episodes therefore reflect not only changes in residence time, but also transient shifts in hydraulic connectivity.

The RES, SDI and RI indicators allow sediment-capture efficiency, depositional stability and secondary redistribution to be evaluated separately. At higher discharges, the contribution of redeposited particles increases, indicating that deposited material more frequently undergoes the cycle of settling, resuspension and redeposition into another zone. This flow-regime dependence is also expressed quantitatively by SDI and RI: during HF, SDI values below 0.5 dominated the lower reservoir and RI locally reached 75–100%, whereas under LF primary deposition prevailed and RI generally remained within the 0–50% range. This is consistent with lithodynamic analyses of bed sediments, which show that transport-equilibrium conditions prevail over a large part of the Włocławek Reservoir, whereas persistent accumulation is concentrated in isolated depressions and low-energy areas (Gierszewski, 2018). Post-depositional hydraulic sorting may enrich shallow and marginal areas in fine fractions, whereas the channel core tends to retain fractions with higher critical shear stresses for entrainment (Van Rijn, 1984; Soulsby, 1997). Under low-flow conditions, higher SDI values indicate greater stabilization of deposited material, allowing neighbouring accumulation patches in FRI and FP to develop into more continuous

https://doi.org/10.5194/egusphere-2026-6675
Preprint. Discussion started: 4 November 2026
© Author(s) 2026. CC BY 4.0 License.

depositional belts. Such mechanisms are widely reported in reservoirs, where resuspension and redeposition strongly influence the final distribution of fine-grained deposits (Bloesch, 1995; Håkanson, 2006).

Wind forcing may further amplify these processes in shallow parts of the Włocławek Reservoir. Previous field-based assessments indicate that, at wind speeds of 8 m s^{-1}, approximately 5–11% of the bed may be affected by resuspension, whereas during storms with wind speeds of 15 m s^{-1} this share may increase to as much as 40% (Gierszewski, 2018). Because wind and surface-wave forcing were not included in the present simulations, the PTM results represent the throughflow-related component of redeposition. Total redeposition, particularly over shallow FP surfaces and locally over former island/bar areas, may therefore be higher during storm events.

The preferential accumulation and redeposition over FRI are consistent with studies emphasizing feedbacks among sedimentation, vegetation and island development in multi-channel or anabranching systems (Gurnell et al., 2001, 2012). In the pre-impoundment Vistula reach, numerous islands and bars formed a laterally structured channel template; their preservation on the reservoir bed explains why FRI remains a key zone of sediment capture and redistribution under present reservoir conditions (Gierszewski et al., 2015; Gierszewski, 2018). According to previous bed-sediment lithodynamic analyses, deposits in former channel-belt and island/bar settings may reflect a combination of suspension-derived deposition and saltation–traction transport, whereas areas outside the channel core are dominated more strongly by suspension-derived fine material (Gierszewski, 2018).

The PTM simulation under unsteady-flow conditions explicitly resolves particles that settle as velocities decrease and are subsequently re-entrained as velocities increase, before migrating farther through the reservoir. Field-based sediment data therefore complement rather than compete with modelling. Together, they support three linked interpretations (i) transport and redeposition occur across much of the reservoir basin; (ii) suspension-derived deposition is most pronounced in middle, lower and marginal low-energy areas; and (iii) legacy-controlled accumulation hotspots over former island/bar surfaces are simultaneously important sediment sinks and zones susceptible to cyclic resuspension.

4.3. Implications for classical reservoir-sedimentation concepts and river–reservoir continuum models

According to the classical three-zone model of reservoir sedimentation—riverine, transitional and lacustrine—depositional intensity and grain-size sorting are expected to follow a primarily longitudinal pattern controlled by decreasing flow velocity and transport capacity along the reservoir axis (Thornton et al., 1990; Morris and Fan, 1998). In the Włocławek Reservoir, this longitudinal gradient is present, but it is substantially modified by inherited morphology. Deposition does not form a simple monotonic downstream or upstream gradient; instead, depositional maxima and grain-size patterns shift among flow scenarios and are locally organized by the preserved thalweg, former channel belt, and former island/bar zones. This produces a mosaic of depositional patches coupled to the velocity field and to inherited planform and bathymetric structures.

The comparison with previously published bed-sediment data further supports this interpretation. In the central sector of the reservoir, modelled maxima in suspended-sediment deposition show spatial correspondence with measured maxima in bed-deposit thickness after several decades of reservoir operation (Fig. 10). This comparison should not be interpreted as a full validation of long-term reservoir infilling by event-scale simulations. Rather, it provides supporting evidence that the same inherited morphological template that organizes event-scale particle routing is also reflected in longer-term patterns of sediment accumulation.

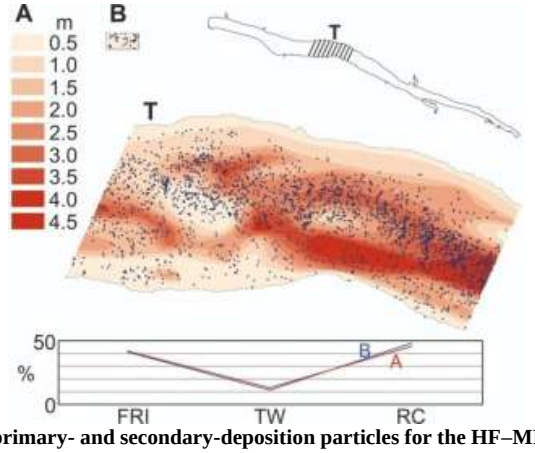


Fig. 10. Distribution of primary- and secondary-deposition particles for the HF–MF–LF scenarios overlaid on the map of measured bed-sediment thickness in the central sector of the Włocławek Reservoir (14–19 km upstream of the dam; reach T) after 50 years of reservoir operation; and comparison of the percentage

https://doi.org/10.5194/egusphere-2026-6675
Preprint. Discussion started: 4 November 2026
© Author(s) 2026. CC BY 4.0 License.

contribution of bed-sediment layer thickness (A) with the percentage contribution of particle counts (B) across morphodynamic zones.

These results imply that the riverine–transitional–lacustrine scheme remains useful as a general longitudinal framework, but should be supplemented by s legacy-controlled component in valley reservoirs with short residence times and well-preserved pre-impoundment morphology. In such systems, sedimentation patterns may be shaped not only by downstream reductions in transport capacity, but also by inherited cross-sectional and planform structures, especially where reservoirs inundate formerly multi-channel or anabranching river reaches (cf. Leopold et al., 1964; Liro et al., 2020).

Trapping efficiency, classically interpreted using Brune's curves as a function of the capacity–inflow ratio (Brune, 1953), is also modified in short-residence-time valley reservoirs by the spatial heterogeneity of the velocity field and by legacy morphology. Modelled suspended-sediment retention increased from 66% during HF to 73% during MF and 94% during LF, demonstrating a strong flow-regime dependence of event-scale sediment trapping within the reservoir. This pattern agrees with broad reservoir-sedimentation generalizations (Dendy and Champion, 1978; Morris and Fan, 1998). However, the spatial pattern of deposition departs from a simple longitudinal gradient. Low deposition in parts of TW and high relative sedimentation efficiency over TW and FRI underscore the importance of cross-sectional controls on flow and sediment routing. Although TW is primarily a transit corridor, its RES is high because the metric relates deposition density to areal share. Deposition within TW is concentrated in a narrow inherited corridor, mainly during lower-energy phases, flow recession and in local low-velocity settings, so its small areal extent yields high relative efficiency. By contrast, FRI may show high local accumulation, but its larger areal extent reduces RES after normalization.

More broadly, these results suggest that predictions derived from the Serial Discontinuity Concept (SDC) may need to account for inherited valley-floor morphology in impounded reaches (Ward and Stanford, 1983). The magnitude and spatial expression of discontinuities may depend not only on dam position within the river network and on altered flow and sediment supply, but also on the geomorphic template preserved on the inundated valley floor. Similarly, in reservoir cascades, legacy-conditioned variability in sediment routing within an upstream reservoir could influence sediment supply to downstream reservoirs and should be considered in future applications of river–reservoir continuum concepts, including the Cascade Reservoir Continuum Concept (CRCC) (Barbosa et al., 1999). These broader implications remain hypotheses for future comparative studies, but the Włocławek Reservoir demonstrates that inherited morphology can be an important internal control on sediment routing within impounded river reaches.

4.4. Indicator-based interpretation of sediment dynamics in inherited morphodynamic zones

The RES, SDI and RI indicators form a complementary suite for quantifying spatial differences in sediment dynamics among inherited morphodynamic zones in valley-type reservoirs (Table 2). RES identifies zones where sediment capture is disproportionately high relative to bed-area share, SDI indicates whether primary deposits are likely to remain stable or be remobilized, and RI quantifies the importance of secondary redistribution. Considered together, these indicators distinguish between sediment-capture hotspots, relatively stable depositional sinks and dynamically reworked sediment zones. The contrast among morphodynamic zones is particularly clear for RES: TW reached a maximum value of 4.10 under LF, FRI reached 2.63 under MF, whereas FP remained consistently below unity, with values of 0.27–0.46 across the three scenarios.

This indicator-based distinction provides a quantitative basis for interpreting the sedimentary functioning of inherited geomorphological units. High RES combined with high SDI indicates zones of efficient and relatively stable sediment storage. In contrast, high RES combined with low SDI or high RI identifies areas where deposition is intense but unstable and therefore susceptible to resuspension and subsequent redistribution. High RI alone points to zones where the final depositional pattern is strongly influenced by secondary transport rather than direct primary settling. Such distinctions are not evident from reservoir-scale trapping efficiency or from a purely longitudinal riverine–transitional–lacustrine classification.

In the Włocławek Reservoir, the FRI and RC–FRI transition zones are particularly important because former island/bar surfaces and adjacent channel-belt margins act both as sediment-capture areas and as sites of secondary redistribution. The TW zone retains a dual function: it remains the principal throughflow corridor, but locally exhibits high relative sedimentation efficiency because deposition is concentrated within a narrow inherited corridor. The FP zone, by contrast, generally shows low relative sedimentation efficiency, but may still act as a marginal fine-sediment sink under specific hydraulic conditions, especially where connectivity with the main flow corridor increases.

These contrasting responses indicate that inherited fluvial landforms are associated with different sedimentary functions within the impounded valley. Former channels and island/bar surfaces do not simply represent preserved elements of pre-impoundment morphology; they also provide a spatial framework within which contemporary sediment capture, remobilization and secondary deposition can be differentiated. The combined interpretation of RES, SDI and RI therefore helps distinguish areas characterized by efficient sediment

https://doi.org/10.5194/egusphere-2026-6675
Preprint. Discussion started: 4 November 2026
© Author(s) 2026. CC BY 4.0 License.

accumulation from those where deposited material is more likely to undergo subsequent redistribution. This distinction is particularly relevant to understanding how the geomorphological legacy of the former river influences the spatial organization of sedimentary processes under altered hydraulic conditions.

From a broader geomorphological perspective, the proposed indicators provide a means of relating inherited landform configuration to contemporary patterns of sediment deposition and redistribution. Their application may support comparative investigations of sedimentary functioning across valley-type reservoirs with different pre-impoundment morphologies and hydrological regimes. However, the indicators describe event-scale sediment dynamics rather than long-term morphological evolution, and their wider applicability requires evaluation in other reservoir systems. Their interpretation should therefore be considered alongside geomorphological reconstruction, sedimentological observations and hydrodynamic modelling.

Beyond their geomorphological significance, RES, SDI and RI may also support targeted sediment sampling, repeated bathymetric surveys and the identification of zones requiring more detailed sediment-dynamics investigation. Such applications remain secondary to their principal role as quantitative descriptors of sedimentary processes and would require additional observational evidence and assessment of site-specific conditions.

4.5. Limitations and future perspectives

The interpretation proposed here should be viewed as an event-scale, process-based assessment of suspended-sediment routing and deposition rather than as a complete reconstruction of the long-term sedimentation history of the Włocławek Reservoir. The simulations were based on three representative hydrological situations and were designed to identify morphology-conditioned sediment-routing patterns under contrasting flow conditions, not to reproduce a continuous seasonal or annual water–sediment sequence. A full-period simulation would require continuous time series of suspended-sediment concentration and grain-size distribution at the inflow boundary, a more complete treatment of wind- and wave-induced resuspension, and substantially higher computational resources. This limitation is particularly important for long-term Lagrangian particle-tracking simulations, in which multiple grain-size fractions and repeated settling–resuspension–redeposition cycles substantially increase computational cost.

The 2-D depth-averaged model (AdH + PTM) does not resolve vertical stratification of velocity and suspended-sediment concentration. For the Włocławek Reservoir, which is characterized by strongly polymictic conditions (Gierszewski, 2018), this is not the primary limitation; however, flocculation can periodically modify the effective settling velocity and mobility of fine fractions (Hill et al., 2000). Because wind and surface-wave forcing were not included, the model may underestimate near-bed shear stress, wind-driven transverse circulation and storm-related resuspension, particularly over shallow FP surfaces and locally over former island/bar areas (Gierszewski, 2018; Jalil et al., 2019). This limitation is less critical for identifying the persistent routing role of the former thalweg and channel belt under throughflow conditions, but it should be considered when interpreting the absolute intensity of resuspension and the stability of fine-grained deposits in shallow marginal zones.

Several data-related limitations should also be noted. The availability and quality of pre-impoundment topography remain constrained because archival maps and bathymetries are scarce and carry uncertainty (Pacina et al., 2020). Suspended-sediment sampling at several verticals and during selected episodes provides representative input for the analysed discharge ranges, but does not encompass all possible hydrological and sediment-supply combinations. Direct extrapolation of the results to the present-day reservoir morphology would require updated bathymetric data, renewed hydrodynamic verification and additional suspended-sediment measurements.

The model does not resolve the vertical grain-size structure of the natural bed-sediment layer or erosion from deeper pre-existing deposits. Simulated resuspension and redeposition therefore refer only to modelled particles that had previously settled during the same event, not to the remobilization of natural bed sediments accumulated before the simulation. Existing bed-sediment data were used only to characterize the sedimentary setting of the reservoir and to compare the modelled depositional patterns with known spatial trends in bottom-sediment composition, depositional zones and sediment thickness.

The present simulations also did not analyse reservoir operation as a separate control on sediment transport. The model scenarios represent observed low-, medium- and high-flow throughflow conditions at the normal pool level, rather than operational variants such as controlled drawdown, sediment flushing, bottom-outlet releases, or hydropower-related short-term water-level fluctuations. Operational effects on sediment remobilization and downstream sediment transfer would require a separate set of scenarios based on detailed dam-operation records and concurrent sediment-monitoring data.

A further limitation is that the study does not include an independent reconstruction of the full long-term sedimentation history of the reservoir. Temporal changes in mean bed elevation and bed slope were therefore not analysed directly, because such an analysis would require comparable multi-temporal bathymetric datasets, explicit correction for dredging-related disturbances, spatially distributed sediment cores, sediment dating, and a complete sediment-budget reconstruction. Although the modelled deposition patterns are compared with previously published empirical data on bottom-sediment properties and sediment thickness, the study does not

https://doi.org/10.5194/egusphere-2026-6675
Preprint. Discussion started: 4 November 2026
© Author(s) 2026. CC BY 4.0 License.

provide a systematic core-based, chronostratigraphic, or repeated-bathymetry analysis of reservoir infilling since impoundment.

Finally, RES, SDI and RI quantify hydromorphological and sediment-dynamic properties of the reservoir bed, but they were not validated against biological communities, habitat-quality metrics or water-quality responses. Therefore, they should be regarded as process-based physical indicators that may support ecological assessment, rather than as direct indicators of ecological status. Future applications should test their relationships with benthic habitat structure, turbidity, nutrient and contaminant dynamics, and biological indicators used in reservoir assessment.

Despite these limitations, the modelling framework provides a coherent basis for quantifying how inherited fluvial morphology controls suspended-sediment routing and deposition in through-flow valley reservoirs. Future work should combine longer hydrological simulations, updated and repeated bathymetric surveys, sediment-core analyses, improved wind-wave forcing and ecological validation to evaluate how event-scale fluvial-memory effects accumulate into decadal-scale reservoir-bed evolution.

5. Conclusions

The results demonstrate that the morphological legacy of the pre-impoundment Vistula River remains clearly expressed in the bed configuration of the Włocławek Reservoir more than five decades after impoundment. The submerged former thalweg, relict-channel belt, island/bar surfaces and inundated floodplain form an inherited geomorphological template associated with distinct contemporary hydrodynamic and sedimentary environments. This persistence indicates that the transformation of a river valley into a reservoir does not necessarily eliminate the geomorphological organization of the former fluvial system.

The AdH–PTM simulations show that the sedimentary expression of this inherited morphology varies with hydrological conditions. Simulated sediment retention increased from 66% during high flow to 73% during medium flow and 94% during low flow. Former thalweg and island/bar zones exhibited disproportionately high relative sediment capture, whereas inundated floodplain surfaces generally showed lower sedimentation efficiency. Higher flows reduced primary-deposit stability and intensified secondary sediment redistribution, demonstrating that spatial patterns of sediment accumulation reflect both inherited morphological differentiation and contemporary hydraulic forcing.

The proposed indicators—Relative Sedimentation Efficiency (RES), Sediment-deposition Stability Index (SDI) and Redeposition Index (RI)—provide complementary quantitative measures of sediment capture, depositional persistence and secondary redistribution within inherited morphodynamic zones. Their combined application reveals that morphodynamic units characterized by high sediment-capture efficiency do not necessarily represent zones of stable sediment storage. This distinction provides an additional perspective on the relationship between preserved fluvial landforms and contemporary sedimentary processes in impounded river valleys.

The study highlights the importance of considering pre-impoundment geomorphology when interpreting sediment-routing and depositional patterns in valley-type reservoirs. The proposed framework offers a basis for examining the sedimentary consequences of fluvial-memory effects in other impounded river systems, although its transferability requires further testing across different geomorphological and hydrological settings. Such comparisons could contribute to a broader understanding of how inherited fluvial landscapes continue to influence sediment dynamics following major anthropogenic alterations of river systems.

Author contributions

PG, Writing – original draft, Writing – review & editing, Methodology, Investigation, Formal analysis, Data curation, Conceptualization, Supervision, Project administration, Funding acquisition, Validation.
WJ, Writing – original draft, Writing – review & editing, Visualization, Methodology, Investigation, Formal analysis, Conceptualization, Project administration, Validation.
MS, Writing – original draft, Writing – review & editing, Visualization, Methodology, Formal analysis, Data curation, Funding acquisition, Validation.
MT, Writing – original draft, Writing – review & editing, Visualization, Methodology, Formal analysis, Data curation, Validation.
PSH, Writing – original draft, Writing – review & editing, Methodology, Formal analysis, Supervision, Funding acquisition.
DS, Writing – review & editing, Methodology, Validation.
MH: Writing – review & editing, Methodology, Investigation, Funding acquisition.
All authors have read and approved the final version of the manuscript and agreed to its submission to Advances in Water Resources.

Competing interest

The authors declare that they have no known competing financial interests or personal relationships that could have appeared to influence the work reported in this paper.

https://doi.org/10.5194/egusphere-2026-6675
Preprint. Discussion started: 4 November 2026
© Author(s) 2026. CC BY 4.0 License.

Disclaimer

Copernicus Publications remains neutral with regard to jurisdictional claims made in the text, published maps, institutional affiliations, or any other geographical representation in this paper. While Copernicus Publications makes every effort to include appropriate place names, the final responsibility lies with the authors. Views expressed in the text are those of the authors and do not necessarily reflect the views of the publisher.

Financial support

This research was funded by the Polish Ministry of Science and Higher Education under agreement no. MNiSW/2025/DAP/841.

Data availability

The data that support the findings of this study are available in an online repository https://doi.org/10.58099/PK/OI8EUU. Other data not presented therein will be made available on request.

References

Amoros, C., Roux, A.L., 1988. Interaction between water bodies within the floodplains of large rivers: function and development of connectivity. Münstersche Geographische Arbeiten 29, 125–130.

Atkinson, E., 1996. The feasibility of flushing sediment from reservoir. Report OD137, HR Wallingford, UK.

Babiński, Z., 1994. Transport rumowiska unoszonego i wleczonego dolnej Wisły w okresie eksploatacji stopnia wodnego Włocławek. Przegląd Geograficzny 67 (3–4), 285–308.

Babiński, Z., 2002. Wpływ zapór na procesy korytowe rzek aluwialnych: ze szczególnym uwzględnieniem stopnia wodnego "Włocławek" [Influence of waterdams on fluvialprocesses: the case of the water dam "Włocławek"]. Akademia Bydgoska im. Kazimierza Wielkiego, Bydgoszcz [Kazimierz Wielki University in Bydgoszcz], 1–185. [In Polish with English summary].

Babiński, Z., 2005. The relationship between suspended and bed load transport in river channels. In: Sediment Transport and Transfer, Proceedings of Symposium S1 Held During the Seventh IAHS Scientific Assembly at Foz do Iguaçu, April 2005, Brazil, 182–188.

Banach, M., 1994. Morfodynamika strefy brzegowej zbiornika Włocławek. IGiPZ PAN, 161.

Barbosa, F.A.R., Padisák, J., Espíndola, E.L.G., Borics, G., Rocha, O., 1999. The cascading reservoir continuum concept (CRCC) and its application to the river Tietê-basin, São Paulo State, Brazil. Theoretical Reservoir Ecology and Its Applications 1, 425–437.

Beevers, L.C., 2003. Morphological sustainability of barrage impoundments. University of Glasgow, PhD thesis. http://encore.lib.gla.ac.uk/iii/encore/record/C__Rb2191041.

Bennett, A., 2006. Lagrangian fluid dynamics. Cambridge University Press.

Berger, R.C., Tate, J.N., Brown, G.L., Savant, G., 2013. Adaptive Hydraulics (USACE).

Bloesch, J., 1995. Mechanisms, measurement and importance of sediment resuspension in lakes. Marine and Freshwater Research 46 (1), 295–304.

Bogucka-Szymalska, M., Magnuszewski, A., 2007. Zastosowanie modelu NCCHE2D do oceny warunków sedymentacji w Jeziorze Włocławskim. Prace i Studia Geograficzne 38, 105–116.

Bortnyk, S., Gierszewski, P. J., Witkowski, K., Szmańda, J. B., 2026. Downstream effects of dam-regulated flow on river-island morphology and lithofacies record in anabranching rivers. Scientific Reports (in press).

Brune, G.M., 1953. Trap efficiency of reservoirs. Trans. Am. Geophys. Union 34, 407–418.

Buffington, J.M., 2012. Changes in channel morphology over human time scales. In: Church, M., Biron, P.M., Roy, A.G. (Eds.), Gravel-bed Rivers: Processes, Tools, Environments. Wiley, Chichester, 435–463.

Buffington, J.M., Montgomery, D.R., 2022. Geomorphic classification of rivers: An updated review. In: Shroder, J.F. (Ed.), Treatise on Geomorphology, 2nd ed., 1143–1190. Academic Press.

Dale, V.H., Beyeler, S.C., 2001. Challenges in the development and use of ecological indicators. Ecological Indicators 1, 3–10.

Dendy, F.E., Champion, W.A., 1978. Sediment deposition in U.S. reservoirs: Summary of data reported through 1975. USDA Misc. Publ. 1362, 84 pp., Agric. Res. Service, U.S. Dept. of Agriculture, Washington, D.C.

Evans, J.E., 2007. Sediment impacts of the 1994 failure of IVEX Dam (Chagrin River, NE Ohio): A test of channel evolution models. Journal of Great Lakes Research 33, 90–102.

Fang, H., He, G., Huang, L., Zhao, C., Wang, J., Han, Y., Gao, Q., Zhang, T., Meng, J., 2024. Altered flow and sediment transport impacts on the ecosystems of Chinese major rivers: An urgent call for eco-fluvial dynamics. River 3, 341–361. https://doi.org/10.1002/rvr2.110.

Gierszewski, P., 2011. Impact of the Włocławek Reservoir on the conditions for the transport of suspended load. GeomorphologiaSlovaca et Bohemica 11 (1), 28–41.

Gierszewski, P., 2018. Hydromorfologiczne uwarunkowania funkcjonowania geoekosystemu Zbiornika Włocławskiego [Hydromorphological conditions of the functioning of the Włocławek reservoir geo-ecosystem]. Prace Geograficzne 268. IGiPZ PAN, Warszawa.

https://doi.org/10.5194/egusphere-2026-6675
Preprint. Discussion started: 4 November 2026
© Author(s) 2026. CC BY 4.0 License.

Gierszewski, P.J., Szmańda, J.B., Luc, M., 2015. Zmiany układu koryt Wisły spowodowane funkcjonowaniem stopnia wodnego 'Włocławek' na podstawie analizy zdjęć lotniczych (summary in English: changes of Vistula riverchannelspatterncaused by Włocławek dam functioningbased on the analysis of aerialphotographs). Przegląd Geograficzny 87, 517–533.

Gierszewski, P.J., Habel, M., Szmańda, J., Luc, M., 2020. Evaluating effects of dam operation on flow regimes and riverbed adaptation to those changes. Sci. Total Environ. 710, 136202.https://doi.org/10.1016/j.scitotenv.2019.136202.

Gurnell, A.M., Bertoldi, W., Corenblit, D., 2012. Changing river channels: The roles of hydrological processes, plants and pioneer fluvial landforms in humid temperate, mixed load, gravel bed rivers. Earth Sci. Rev. 111, 129–141.

Gurnell, A.M., Petts, G.E., Hannah, D.M., Smith, B.P.G., Edwards, P.J., Kollmann, J., Ward, J.V., Tockner, K., 2001. Riparian vegetation and island formation along the gravel-bed Fiume Tagliamento, Italy. Earth Surface Processes and Landforms 26 (1), 31–62.

Habel, M., 2013. Dynamics of the Vistula River channel deformations downstream of Włocławek Reservoir. KazimierzWielki University Press, Bydgoszcz.

Hachaj, P.S., 2013. The 'River Memory' Effect: An Attempt to Understand and Model it. In: Rowiński, P. (Ed.), Experimental and Computational Solutions of Hydraulic Problems, GeoPlanet: Earth and Planetary Sciences. Springer, Berlin, Heidelberg. https://doi.org/10.1007/978-3-642-30209-1_22.

Hachaj, P.S., 2018. Preliminary results of applying 2D hydrodynamic models of water reservoirs to identify their ecological potential. Pol. J. Environ. Stud. 27 (5).

Hachaj, P.S., Gierszewski, P., Juśkiewicz, W., Habel, M., Szlapa, M., Tutro, M., Strzelecki, D., Kaszubski, M., 2024. The ADDRESS of a grain: Sediment particle tracking as an approach to assessing ecosystem quality in dammed reservoirs. Science of the Total Environment 957, 177511.

Hachaj, P.S., Szlapa, M., Tutro, M., 2015. Numerical modelling of sub-glacial flow in a retention reservoir. Environ. Eng. Ser. 1-´S/2015, 37.

Hamidifar, H., Nones, M., Rowinski, P.M., 2024. Flood modeling and fluvial dynamics: A scoping review on the role of sediment transport. Earth-Science Reviews 253, 104775.

Herrera-Díaz, I.E., Torres-Bejarano, F.M., Moreno-Martínez, J.Y., Rodriguez-Cuevas, C., Castañeda, C., 2017. Light particle tracking model for simulating bed sediment transport load in river areas. Mathematical Problems in Engineering, 1679257. https://doi.org/10.1155/2017/1679257.1026.

Hill, P.S., Milligan, T.G., Geyer, W.R., 2000. Controls on effective settling velocity of suspended sediment in the Eel River flood plume. Continental Shelf Research 20 (16), 2095–2111.

Iliopoulou, T., Aguilar, C., Arheimer, B., Bermúdez, M., Bezak, N., Ficchì, A., Koutsoyiannis, D., Parajka, J., Polo, M.J., Thirel, G., Montanari, A., 2019. A large sample analysis of European rivers on seasonal river flow correlation and its physical drivers. Hydrol. Earth Syst. Sci. 23, 73–91. https://doi.org/10.5194/hess-23-73-2019.

Jalil, A., Li, Y., Zhang, K., Gao, X., Wang, W., Khan, H.O.S., Pan, B., Ali, S., Acharya, K., 2019. Wind-induced hydrodynamic changes impact on sediment resuspension for large, shallow Lake Taihu, China. International Journal of Sediment Research 34 (3), 205–215. https://doi.org/10.1016/j.ijsrc.2018.11.003.

Juracek, K.E., 2015. The aging of America's reservoirs: in-reservoir and downstream physical changes and habitat implications. JAWRA Journal of the American Water Resources Association 51 (1), 168–184.

Ke, Y., 2021. Source, transport, and fate of particulate organic carbon in the largest Chinese rivers [PhD Thesis]. Université Paris-Saclay. Retrieved from https://theses.hal.science/tel-03793807v1.

Keith, M.K., Wallick, J.R., Schenk, L.N., Stratton Garvin, L.E., Gordon, G.W., Bragg, H.M., 2024. Reservoir evolution, downstream sediment transport, downstream channel change, and synthesis of geomorphic responses of Fall Creek and Middle Fork Willamette River to water years 2012–18 streambed drawdowns at Fall Creek Lake, Oregon. U.S. Geological Survey Scientific Investigations Report 2023–5135, 155 p. https://doi.org/10.3133/sir20235135.

Kurtz, J.C., Jackson, L.E., Fisher, W.S., 2001. Strategies for evaluating indicators based on guidelines from the Environmental Protection Agency's Office of Research and Development. Ecological Indicators 1, 49–60.

Lai, Y.G., Huang, J., Greimann, B.P., 2024. Hydraulic flushing of sediment in reservoirs: Best practices of numerical modeling. Fluids 9 (2), 38.

Lee, S., Wolberg, G., Shin, S.Y., 1997. Scattered data interpolation with multilevel B-splines. IEEE Trans. Vis. Comput. Graph. 3 (3), 228–244.https://doi.org/10.1109/2945.620490.

Leopold, L.B., Wolman, M.G., Miller, J.P., 1964. Fluvial processes in geomorphology. Freeman, San Francisco, CA, 522 pp.

Liro, M., Ruiz-Villanueva, V., Mikuś, P., Wyżga, B., Castellet, E.B., 2020. Changes in the hydrodynamics of a mountain river induced by dam reservoir backwater. Science of the Total Environment 744, 140555.

https://doi.org/10.5194/egusphere-2026-6675
Preprint. Discussion started: 4 November 2026
© Author(s) 2026. CC BY 4.0 License.

Liu, C.C.H., Tsai, C.W., Huang, Y.Y., 2021. Development of a backward–forward stochastic particle tracking model for identification of probable sedimentation sources in open channel flow. Mathematics 9 (11), 1263. https://doi.org/10.3390/math9111263.

Livers, B., Wohl, E., 2016. Sources and interpretation of channel complexity in forested subalpine streams of the Southern Rocky Mountains. Water Resources Research 52(5), 3910–3929. https://doi.org/10.1002/2015WR018306.

Livers, B., Wohl, E., Jackson, K.J., Sutfin, N.A., 2018. Historical land use as a driver of alternative states for stream form and function in forested mountain watersheds of the Southern Rocky Mountains. Earth Surface Processes and Landforms 43(3), 669–684. https://doi.org/10.1002/esp.4275.

Livers, B., Snyder, N.P., 2025. Legacy sediment: A conceptual model and perspective on the role of dams. Earth Surface Processes and Landforms 50(4), e70044. https://doi.org/10.1002/esp.70044.

Łajczak, A., 1999. Współczesny transport i sedymentacja materiału unoszonego w Wiśle i głównych dopływach. Monografie Komitetu Gospodarki Wodnej PAN 15, Warszawa.

MacDonald, N.J., Davies, M.H., Zundel, A.K., Howlett, J.D., Demirbilek, Z., Gailani, J.Z., Lackey, T.C., Smith, J., 2006. PTM: Particletracking model. Report 1: Model theory, implementation, and example applications.

Masteller, C.C., Finnegan, N.J., Turowski, J.M., Yager, E.M., Rickenmann, D., 2019. History-dependent threshold for motion revealed by continuous bedload transport measurements in a steep mountain stream. Geophysical Research Letters 46, 2583–2591. https://doi.org/10.1029/2018GL081325.

Mączka, N., Hachaj, P.S., Szlapa, M., 2024. Implementation of the numerical model of an active bed for the Wloclawek Reservoir. Geoinformatica Polonica 23, 17–24.

McCartney, M.P., Sullivan, C., Acreman, M.C., 2000. Ecosystem impacts of large dams. Background Paper No. 2 prepared for IUCN/UNEP/WCD. Center for Ecology and Hydrology, Wallingford, UK.

Meybeck, M., Laroche, L., Dürr, H.H., Syvitski, J.P.M., 2003. Global variability of daily total suspended solids and their fluxes in rivers. Glob. Planet. Chang. 39 (1–2), 65–93.

Morris, G.L., Fan, J., 1998. Reservoir sedimentation handbook: Design and management of dams, reservoirs and watersheds for sustainable use. McGraw-Hill, New York.

Pacina, J., Lenďáková, Z., Štojdl, J., MatysGrygar, T., Dolejš, M., 2020. Dynamics of sediments in reservoir inflows: A case study of the Skalka and Nechranice reservoirs, Czech Republic. ISPRS International Journal of Geo-Information 9 (4), 258.

Pringle, C.M., 2001. Hydrologic connectivity and the management of biological reserves: A global perspective. Ecological Applications 11 (4), 981–998.

Savant, G., Berger, R.C., 2012. Adaptive time stepping–operator splitting strategy to couple implicit numerical hydrodynamic and water quality codes. J. Environ. Eng. 138 (9), 979–984.

Sedláček, J., Bábek, O., Kielar, O., 2016. Sediment accumulation rates and high-resolution stratigraphy of recent fluvial suspension deposits in various fluvial settings, Morava River catchment area, Czech Republic. Geomorphology 254, 73–87.

Sedláček, J., Bábek, O., Grygar, T.M., Lenďáková, Z., Pacina, J., Štojdl, J., Hošek, M., Elznicová, J., 2022. A closer look at sedimentation processes in two dam reservoirs. Journal of Hydrology 605, 127397.

Sidorchuk, A., 2003. Floodplain sedimentation: Inherited memories. Global and Planetary Change 39, 13–29.

Słowik, M., Dezső, J., Marciniak, A., Tóth, G., Kovács, J., 2018. Evolution of river planforms downstream of dams: Effect of dam construction or earlier human-induced changes? Earth Surface Processes and Landforms 43 (10), 2045–2063. https://doi.org/10.1002/esp.4371.

Soulsby, R., 1997. Dynamics of marine sands. Thomas Telford Publishing. https://doi.org/10.1680/doms.25844.

Stauch, G., Dörwald, L., Esch, A., Walk, J., 2024. 115 years of sediment deposition in a reservoir in Central Europe: Topographic change detection. Earth Surface Processes and Landforms 49 (2), 582–600. https://doi.org/10.1002/esp.5722600.

Szmańda, J.B., Gierszewski, P.J., Habel, M., Luc, M., Witkowski, K., Bortnyk, S., Obodovskyi, O., 2021. Response of the Dnieper river fluvial system to the river erosion caused by the operation of the Kaniv hydro-electric power plant (Ukraine). Catena, 202, 105265.

Tate, J., Gunkel, B., Rosati, J., Sanchez, A., Ganesh, N., Pratt, T., Wood, E., Thomas, R., 2014. Houston-Galveston Navigation Channel Shoaling Study. Engineer Research and Development Center Vicksburg MS Coastal and Hydraulics Lab, 154 pp.

Thornton, K.W., Kimmel, B.L., Payne, F.E., 1990. Reservoir limnology: Ecological perspectives. John Wiley and Sons, New York, 246 pp.

Timchenko, V., Korzhov, Ye., Huliaieva, O., Batoh, S., 2015. Dynamics of environmentally significant elements of hydrological regime of the Lower Dnieper section. Hydrobiological Journal 51, 75–83. https://doi.org/10.1615/HydrobJ.v51.i6.90.

Tutro, M. 2026. “Simulation Videos of Suspended Sediment Transport in the Włocławek Reservoir.” Cracow University of Technology, Version 1. https://doi.org/10.58099/PK/OI8EUU

https://doi.org/10.5194/egusphere-2026-6675
Preprint. Discussion started: 4 November 2026
© Author(s) 2026. CC BY 4.0 License.



Tutro, M., Hachaj, P.S., Szlapa, M., Gierszewski, P., Habel, M., Juśkiewicz, W., Mączka, N., 2022. Implementation of the AdH hydrodynamic model on the Włocławek Reservoir. Geogr. Pol. 95 (4), 371–386. https://doi.org/10.7163/GPol.0241.

Ward, J.V., Stanford, J.A., 1983. The serial discontinuity concept of lotic ecosystems. In: Dynamics of Lotic Ecosystems. Fontaine, T.D., Bartell, S.M. (Eds.). Ann Arbor Science, Ann Arbor, MI, 29–42.

Wohl, E., 2015. Legacy effects on sediments in river corridors. Earth-Science Reviews 147, 30–53.

Wohl, E., 2019. Forgotten legacies: Understanding and mitigating historical human alterations of river corridors. Water Resources Research 55 (7), 5181–5201. https://doi.org/10.1029/2018WR024433.

Wohl, E., Rathburn, S., Dunn, S., Iskin, E., Katz, A., Marshall, A., Means-Brous, M., Scamardo, J., Triantafillou, S., Uno, H., 2024. Geomorphic context in process-based river restoration. River Research and Applications 40 (3), 322–340. https://doi.org/10.1002/rra.4236.

Van Rijn, L.C., 1984. Sediment transport, part I: bed load transport. Journal of Hydraulic Engineering 110 (10), 1431–1456.

Venteris, E.R., May, C.J., Hewitt, J., 2014. Cost-effective mapping of benthic habitats in inland reservoirs through split-beam sonar, indicator kriging, and historical geologic data. PLoS ONE 9 (4), e95940.